Scilight

Regenerative Medicine and Dentistry
https://www.sciltp.com/journals/rmd



Review

Check for updates

Engineering Electro-Regenerative Microenvironment for Bone Repair: Advances in Electroactive Biomaterials

Hongye Yang [1,†], Ruobing Liang [1,†], Jipeng Zhang [2], Yihao Liu [1], Kiho Cho [3], Yaning Zhao [1,*], Ang Lu [2,*] and Cui Huang [1,*]

[1] State Key Laboratory of Oral & Maxillofacial Reconstruction and Regeneration, Key Laboratory of Oral Biomedicine Ministry of Education, Hubei Key Laboratory of Stomatology, School & Hospital of Stomatology, Wuhan University, Wuhan 430079, China
[2] Hubei Engineering Center of Natural Polymer-Based Medical Materials, Key Laboratory of Biomedical Polymers of Ministry of Education, College of Chemistry and Molecular Sciences, Wuhan University, Wuhan 430072, China
[3] Division of Applied Oral Sciences and Community Dental Care, Faculty of Dentistry, The University of Hong Kong, Hong Kong SAR 999077, China
* Correspondence: zyn2016@whu.edu.cn (Y.Z.); anglu@whu.edu.cn (A.L.); huangcui@whu.edu.cn (C.H.)
† These authors contributed equally to this work.

How To Cite: Yang, H.; Liang, R.; Zhang, J.; et al. Engineering Electro-Regenerative Microenvironment for Bone Repair: Advances in Electroactive Biomaterials. *Regenerative Medicine and Dentistry* **2026**, *3*(4), 16. https://doi.org/10.53941/rmd.2026.100016

Received: 30 August 2026
Revised: 15 October 2026
Accepted: 21 October 2026
Published: 3 November 2026

Abstract: As a quintessential hard tissue in human, bone represents a masterpiece of biomineralization, with mineralized collagen fibrils serving as its fundamental building blocks. During the natural repair processes of bone, endogenous bioelectric fields generated by mineralized collagen have been demonstrated to promote tissue regeneration by modulating cellular behaviors and signal transduction. Inspired by these physiological mechanisms, increasing research efforts have focused on engineering electroactive biomaterials to modulate local bioelectrical cues and establish regenerative microenvironments conducive to bone repair. In this context, we propose the concept of the electro-regenerative microenvironment (ERM), which emphasizes the regulation of interconnected biological processes, including antibacterial activity, immunomodulation, angiogenesis, neurogenesis, and osteogenesis, through bioelectrical cues mediated by electroactive biomaterials. This review first discusses the nature of endogenous electric fields in bone and the electroactive, electrosensitive, and electro-responsive properties of hard tissues. Electroactive biomaterials are then discussed according to their primary electrical functions, with a focus on conductive and piezoelectric materials, while also considering triboelectric and other relevant electroactive systems. Subsequently, the mechanisms by which these materials contribute to the establishment and regulation of the ERM are summarized. Emerging trends, future research directions, and clinical translational challenges are also discussed. Overall, this review highlights recent advances in electroactive biomaterials and provides insights for designing next-generation biomaterials that engineer ERM for bone repair.

Keywords: bone regeneration; electroactivity; conductivity; piezoelectricity; endogenous bioelectricity

1. Introduction

Bone is a rigid and highly specialized organ of vertebrates that not only provides structural support and protection for the body but also plays essential roles in mineral storage, hematopoiesis, and calcium-phosphorus metabolism [1]. The occurrence of bone defects can result from trauma, infection, tumors, metabolic diseases, and congenital abnormalities, all of which compromise the integrity and structure of bone. Bone defects impair patients'

Copyright: © 2026 by the authors. This is an open access article under the terms and conditions of the Creative Commons Attribution (CC BY) license (https://creativecommons.org/licenses/by/4.0/).
Publisher's Note: Scilight stays neutral with regard to jurisdictional claims in published maps and institutional affiliations.

daily life and motor functions, may lead to pain and infection, and in severe cases, cause limb disability, posing significant physical, psychological, and socioeconomic burdens [2]. With the exacerbation of global aging issues and the increasing incidence of traumatic injuries in regional conflicts, the clinical demand for effective bone repair strategies continues to escalate.

At present, autologous bone grafting remains the gold standard for the treatment of critical-sized bone defects. However, its application is limited by insufficient graft availability and the potential complications from additional surgeries. Allogeneic and xenogeneic bones, while more accessible, introduce risks of immune rejection and disease transmission [3]. Consequently, the development of bioactive materials for bone tissue engineering (BTE) has become a major research focus. Since Crane et al. systematically proposed the concept and methodology of BTE in 1995, the field has rapidly advanced. The basic method of BTE is to combine biologically active bone tissue cells with biomaterials in accordance with the principles of biology and engineering, and then achieve bone tissue repair through *in vitro* or *in vivo* construction methods [4]. Scaffold materials, stem cells, and growth factors constitute the "three essential elements" of BTE, working synergistically to guide and accelerate the regenerative cascade. Among them, the design of scaffold materials is particularly critical and is currently a hot topic in interdisciplinary research. Scientists are striving to develop multifunctional scaffold materials capable of promoting osteogenesis, angiogenesis, neurogenesis, and immunomodulation to achieve precise regulation of the bone regeneration process.

Bone itself is a masterpiece of biomineralization. Its highly ordered hierarchical architecture and unique physicochemical properties have inspired numerous biomimetic strategies for hard-tissue repair. Structurally, bone consists of 30% organic matrix (primarily type I collagen) and 70% inorganic minerals (mainly hydroxyapatite). The basic structural unit, mineralized collagen fibrils, combines the tensile strength of collagen's triple-helical structure with the stiffness of hydroxyapatite crystals [5,6]. Under mechanical loading, this organic–inorganic composite generates surface charges through deformation, producing endogenous bioelectric signals. These piezoelectric and electrophysiological properties play essential roles in bone growth, remodeling, and repair [7].

By emulating nature and deriving inspiration from the sophisticated structures and intrinsic bioelectric properties of natural bone, researchers gain an inexhaustible source of ideas for developing biomimetic materials for hard tissue repair. Electroactive biomaterials broadly refer to materials capable of conducting electrical charges, responding to electrical stimuli, or generating electrical signals in response to external stimuli. Based on their primary electrical functions, these materials can be broadly discussed as charge-conducting systems [8] and electrical signal-generating systems. The former primarily facilitate electronic or ionic charge transport, whereas the latter generate electrical signals through energy-conversion mechanisms, such as piezoelectricity [7,9,10], triboelectricity [11–13], and pyroelectricity [14]. Ferroelectric materials [15], characterized by switchable spontaneous polarization, also represent an important class of electroactive materials, although ferroelectricity may coexist with piezoelectricity and pyroelectricity. These electrical properties are not necessarily mutually exclusive and may be integrated within multifunctional biomaterial systems. Currently, a wide variety of electroactive biomaterials have begun to make their mark in the biomedical field. For example, electrode fabrication [16,17], wound care [18,19], and sensors [20] all rely on the application of conductive biomaterials. Sensors [21], tissue regeneration platforms [22,23], and drug delivery systems [24,25] frequently incorporate piezoelectric and triboelectric biomaterials as core components. For the purposes of skin cancer detection and medical imaging, pyroelectric biomaterials serve as effective functional materials. In the realm of neural engineering, ferroelectric biomaterials have been further exploited in neural implants, enabling the dual functions of recording and stimulating electrical activity in the brain [26]. By meticulously classifying the wide variety of electroactive biomaterials and selecting specific biomaterials suitable for bone repair, we can more precisely meet the personalized demands of hard tissue defects, which not only holds profound scientific value but also demonstrates significant practical importance in clinical applications.

Beyond serving as conductive or piezoelectric scaffolds, electroactive biomaterials are increasingly recognized as platforms for reconstructing the local regenerative microenvironment through bioelectrical cues [27]. Bone regeneration is not a single osteogenic event but a highly coordinated process involving antibacterial regulation, immune modulation, angiogenesis, neurogenesis, and osteogenesis. These processes are tightly coupled and collectively determine the outcome of bone repair [28,29]. Therefore, rather than focusing solely on osteogenesis, it is more appropriate to consider how electroactive biomaterials regulate the overall regenerative microenvironment. In this context, we propose the concept of an electro-regenerative microenvironment (ERM), defined as a bioelectrically regulated local microenvironment engineered by electroactive biomaterials, in which electrical cues modulate cellular behavior, intercellular communication, and tissue regeneration processes in a spatially and temporally coordinated manner. This concept shifts the design strategy of electroactive biomaterials from single-function osteogenic scaffolds toward microenvironment-engineering platforms for functional bone regeneration.

Accordingly, this review first introduces the endogenous bioelectricity and piezoelectricity of bone, which provide the biological basis for electroactive biomaterials. Next, the classification and fabrication strategies of electroactive biomaterials are discussed. Subsequently, the roles of electroactive biomaterials in engineering the ERM are summarized, including antibacterial regulation, immunomodulation, angiogenesis, neurogenesis, and osteogenesis. Finally, future research directions and clinical translational challenges of electroactive biomaterials for bone repair are discussed (Figure 1).

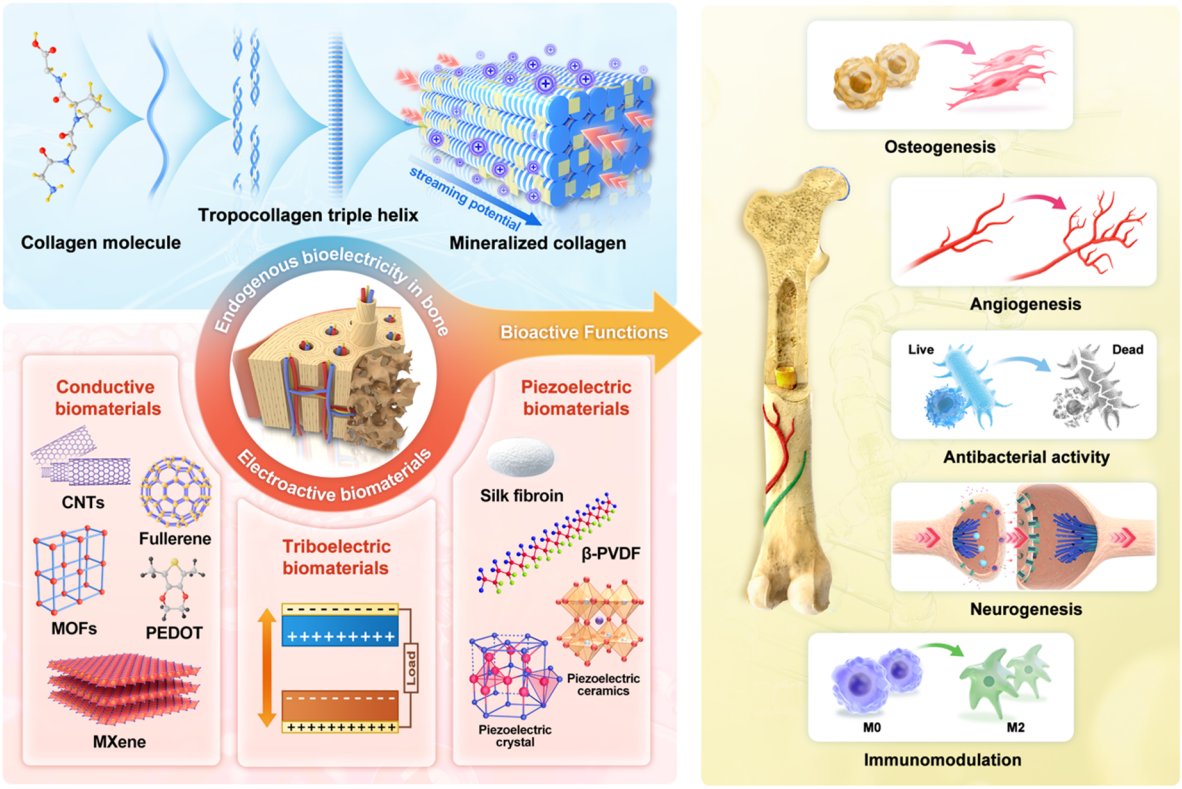


Figure 1. Schematic illustration of endogenous bioelectricity in bone, representative electroactive biomaterial systems, including conductive, piezoelectric, and triboelectric systems, and their bioactive functions for bone repair and regeneration. Piezoelectric responses and streaming potentials are distinct mechanisms that may contribute to mechanically induced bioelectrical signals in bone. Piezoelectricity arises from deformation-induced polarization of the solid collagen structure, whereas streaming potentials result from pressure-driven transport of mobile ions within the electrical double layer along charged pore or channel surfaces.

2. Endogenous Bioelectricity and the Piezoelectricity of Bone

In 1848, physiologist Du Bois-Reymond first proposed the concept of endogenous electric fields, sparking an upsurge in research on bioelectricity [30]. Endogenous electric fields exist in biological tissues and organs as naturally occurring micro-direct current fields within organisms. They serve as the foundation for bioelectric signal transduction and play a crucial role in various physiological processes [31–33]. At the molecular level, amino acid molecules generate opposite surface charges due to their asymmetric molecular structure, exhibiting structural dependence [22]. At the cellular level, ion channels and ion pumps generate and maintain the transmembrane potential (Vm). When tissue injury occurs, fluctuations in V_m regulate specific cellular behaviors including proliferation, migration, differentiation, and Golgi apparatus polarization [32]. At the tissue level, cells are not only regulated by their own V_m but also modulate the V_m of adjacent cells through gap junctions. Such electrical coupling contributes to symmetric organogenesis during embryonic development [34] and orchestrates intercellular communication, stem cell homing, and other biological behaviors critical for tissue repair [35].

Bone exhibits multiple bioelectric properties. Firstly, bone is intrinsically piezoelectric. Biological piezoelectricity is one of the sources of endogenous electric fields. The piezoelectricity of bone was first reported by Fukada in 1957 [36], with a piezoelectric coefficient of 0.22 pC N^{-1}. This phenomenon is closely related to the structural organization of mineralized collagen fibrils. Under shear forces, the sliding of collagen fibrils compresses the non-centrosymmetric quasi-hexagonal lattice of amino acid molecules, causing charge separation and generating

piezoelectric potentials. The transmission of electrical signals within the bone microenvironment facilitates the nucleation and crystallization of hydroxyapatite [7]. Secondly, bone exhibits pyroelectric properties. It refers to the capacity to generate electricity via polarization of negative and positive charges in response to temperature fluctuations [37]. The mutual conversion between lighter and heavier residues results in the distortion in triple helix structure of collagen, which renders pyroelectricity to natural living bone [38]. Thirdly, ferroelectricity is characterized by spontaneous polarization that can be reversibly switched by an applied electric field. This polarization switching should not be equated with changes in collagen fibril orientation. Ferroelectric behavior has been reported in dry cortical bone [39]. However, this finding should not be directly extrapolated to physiologically hydrated bone, and its physiological significance in living bone remains to be established. Lastly, in addition to the piezoelectric response of the solid matrix, mechanical loading can generate pressure gradients that drive interstitial ionic fluid through charged pores and channels in bone. The resulting transport of mobile ions within the electrical double layer produces streaming potentials, an electrokinetic mechanism distinct from piezoelectricity. Both mechanisms may contribute to bone bioelectrical responses, with their relative contributions depending on hydration and experimental conditions. Beyond these intrinsic properties, biological response of hard tissues can also be improved by external electrical stimulation, offering an additional pathway to modulate bone regeneration [40].

3. Classification of Electroactive Biomaterials

With growing recognition of the importance of bioelectricity in tissue regeneration, electroactive biomaterials have attracted considerable attention as platforms for modulating local electrical cues. As outlined in the Introduction, these materials can be broadly distinguished according to their primary electrical functions, including charge conduction and electrical signal generation. Conductive biomaterials primarily facilitate the transport of electronic or ionic charges, whereas electrical signal-generating systems can convert external stimuli into electrical outputs through piezoelectric, triboelectric, or pyroelectric effects. Ferroelectricity, characterized by switchable spontaneous polarization, represents an additional electroactive property that may overlap with piezoelectricity and pyroelectricity.

Given their extensive investigation and relevance to bone tissue engineering, this section focuses on two representative categories: conductive and piezoelectric biomaterials (Figure 2). Conductive biomaterials are discussed in terms of their compositions, electrical properties, fabrication strategies, and applications in bone regeneration (Table 1). Piezoelectric biomaterials are subsequently classified according to their material compositions, including inorganic, organic, and organic–inorganic composite systems (Table 2). Triboelectric systems and their applications in bone repair are further discussed in Section 4.5.3 (Table 3).

3.1. Conductive Biomaterials

Conductive biomaterials, as a fundamental subclass of electroactive biomaterials, are characterized by their intrinsic ability to facilitate the directional movement of electrical charges—whether electrons or ions—under an applied electric field. Unlike piezoelectric biomaterials, which generate electrical polarization in response to mechanical stimuli, conductive biomaterials primarily facilitate electronic or ionic charge transport. By providing pathways for the transmission and distribution of endogenous or externally applied electrical signals, these materials can contribute to the regulation of the local electrical microenvironment. This charge-transport capability enables conductive biomaterials to modulate the local electrical microenvironment, thereby influencing cellular behaviors relevant to tissue regeneration. Based on compositional differences, conductive biomaterials are broadly classified into several categories: carbon-based biomaterials, metal, and conductive polymers.

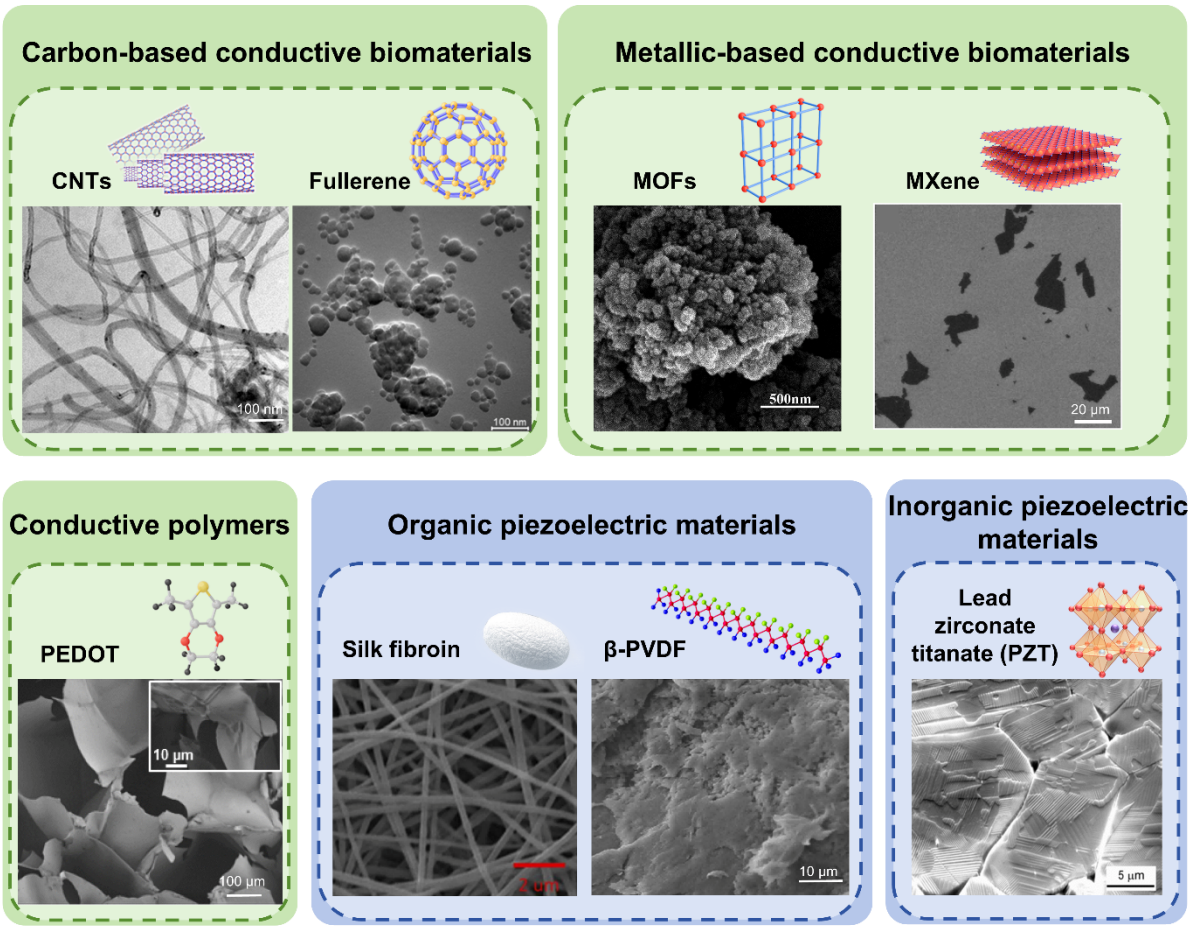


Figure 2. Representative conductive and piezoelectric biomaterials: structural schematics and microscopic morphologies. Carbon-based conductive biomaterials include carbon nanotubes (CNTs) and fullerenes, with representative microscopic images from Refs. [41] with permission of Elsevier, © 2003 and Refs. [42] with permission of American Chemical Society, © 2015. The upper-right section presents metal-organic frameworks (MOFs) and MXene, with representative microscopic images from Refs. [43] with permission of The Royal Society of Chemistry, © 2016 and Ref. [44] with permission of Springer Nature, © 2024. Conductive polymers are represented by poly(3,4-ethylenedioxythiophene) (PEDOT), while the corresponding scaffold micrograph shows a silane-modified gelatin-PEDOT:PSS composite from Ref. [45] with permission of The Royal Society of Chemistry, © 2023. Organic piezoelectric materials include silk fibroin and β-phase poly (vinylidene fluoride) (β-PVDF), with representative microscopic images from Refs. [46] with permission of Elsevier, © 2024 and Ref. [47] with permission of MDPI, © 2020. The inorganic piezoelectric ceramic micrograph shows lead zirconate titanate (PZT), a lead-containing material, from Ref. [48] with permission of John Wiley and Sons, © 2008. The PZT micrograph is included to illustrate ceramic microstructure and does not imply suitability for bone repair or biomedical applicability comparable to that of lead-free $BaTiO_3$.

3.1.1. Carbon-Based Conductive Biomaterials

Carbon-based conductive biomaterials are primarily composed of carbon elements, ranging from 3D graphite and diamond, 2D graphene, graphene oxide (GO), reduced graphene oxide (rGO), 1D carbon nanotubes (CNTs), to 0D graphene oxide quantum dots (GOQDs), fullerenes, and nanodiamonds [49–52]. The anisotropy, size, mechanical properties, and surface modifiability of carbon endow them with diverse properties. Among these, graphene and CNTs are widely used in tissue engineering due to their excellent mechanical properties, chemical stability, large specific surface area, and high electrical conductivity [53,54].

In 2004, Novoselov first described graphene as a single-crystal graphite film and defined it as a 2D semi-metal with high quality, environmental stability, metallic characteristics, and strong electric field effects [55]. However, graphene has been reported to pose substantial cytotoxicity in biomedical applications. The toxicity mechanisms associated with graphene-family nanomaterials (GFNs) were systematically reviewed by Ou et al. For example, GFNs may cause acute inflammatory responses and chronic damage in lungs. Specifically, GO and

rGO reduce cell adhesion, induce apoptosis, and enter lysosome, mitochondria, nuclei, and cytoplasm [56]. Therefore, to address these limitations and incorporate multifunctionality, graphene and its derivatives are frequently integrated into biocompatible composite materials. Within such composite materials, graphene often serves as a "reinforcing agent" to improve mechanical properties and electrical conductivity [57–59]. Currently, graphene is also commonly used in BTE to fabricate conductive scaffolds capable of transmitting endogenous bioelectric signals [60,61].

Structurally, carbon nanotubes can be divided into single-walled carbon nanotubes (SWCNTs) and multi-walled carbon nanotubes (MWCNTs), both characterized by a large surface area. Carbon nanotubes exhibit excellent mechanical, thermal and electrical properties [62]. They are often used to enhance the mechanical properties of biomaterials and serve as scaffolds for guided bone regeneration (GBR). Unlike graphene, functionalized multi-walled carbon nanotubes (fMWCNTs) can maintain high electrical conductivity even after multiple surface modifications due to their multi-layered structure. Moreover, fMWCNTs enhance the interaction force between polymer matrices, achieving synergistic enhancements in conductivity and mechanical performance. However, CNTs also face issues of cytotoxicity. They were among the first nanomaterials added to the SIN (Substitute It Now) list by the Swedish non-profit organization "International Chemical Secretariat" [63]. Although some studies have shown that surface functionalization of CNTs can improve cytocompatibility [64], their biosafety should be rigorously evaluated before biomedical applications.

3.1.2. Metallic-Based Conductive Biomaterials

Metal and metal oxides, including gold, silver, zinc, titanium, strontium, magnesium, copper, and platinum, can be engineered into diverse forms of bone repair materials.

At the macroscopic level, unlike bulk materials formed by dense metals, porous metal scaffolds possess an elastic modulus that matches the hard tissue of human. They can reduce the occurrence of bone resorption when employed in bone tissue engineering [65]. Additionally, they exhibit good biocompatibility, promoting cell attachment, growth, proliferation, and differentiation, as well as facilitating the transport of nutrients and metabolic waste. Studies have shown that a porosity of 88.8% results in optimal cell condition and quantity [66].

At the microscopic level, nanoparticles represent a prominent category of metallic-based biomaterials. Gold and silver nanoparticles not only exhibit optical, electrical, and photothermal properties [67,68], but also demonstrate antibacterial activity, high osteoconductivity, cytocompatibility, and pro-proliferative properties in biological systems [69,70]. making them widely used in hard tissue repair. Metal-organic frameworks (MOFs) are porous crystalline materials formed by the self-assembly of metal ions or metal clusters with organic ligands through coordination bonds. Their unique crystal structure endows them with an ultra-high specific surface area, providing abundant sites for cell adhesion and proliferation. In terms of electroactivity, certain MOF materials exhibit excellent conductivity, which stems from the electron conduction pathways between their internal metal nodes and organic ligands. Studies have confirmed that modified MOFs can self-assemble on demineralized dentin surfaces, forming protective coatings that significantly enhance the mechanical strength and resistance to proteolysis of the dentin matrix [71]. Therefore, MOFs hold promise as multifunctional materials for hard tissue repair.

MXene is a novel class of two-dimensional transition metal carbides, nitrides, and carbonitrides, featuring good conductivity, excellent mechanical strength, and a high surface area. Since its first discovery in 2011, MXene has attracted widespread attention in energy storage, catalysis, and biomedical applications due to its unique structure and properties [72]. MXene can provide electrical stimulation to promote the growth and differentiation of stem cells. Additionally, the excellent biocompatibility and tunable surface functionalization of MXene enable it to be combined with other biomaterials, such as ceramics and polymers, to form multifunctional scaffold systems that support bone/dentin regeneration [73]. Beyond "A + B" simple physical mixing, metallic conductive materials can also co-assemble with matrix materials to achieve structural and functional integration [74,75]. As functional materials capable of surface modification and material assembly, they are often used to modify scaffold materials, synergistically enhancing hard tissue repair effects [76].

The clinical application of metallic conductive biomaterials in hard tissue repair is constrained by several inherent limitations, including non-degradability, potential cytotoxicity, and weak osseointegration ability [77]. Nowadays, researchers are turning their attention to degradable metal-based bone repair materials with acceptable biocompatibility [78], such as magnesium alloys and zinc alloys. Additionally, although metallic-based biomaterials generally possess antibacterial properties, aseptic inflammation remains a significant concern to their biosafety, adversely affecting their long-term prognosis as clinical biomaterials [79]. Therefore, in the future, surface modification and advanced fabrication techniques can be employed to develop metallic-based conductive

biomaterials that match the degradation rate of bone remodeling, feature gradient architectures, and exhibit improved biocompatibility.

3.1.3. Conductive Polymers

Conductive polymer have conjugated π-bonds, capable of electron transitions and exhibiting high conductivity [80]. Due to their inherent flexibility and versatility, Conductive polymer frequently appear in biomedical-related research. Conductive polymers include polypyrrole (PPy), polyaniline (PANi), polythiophene (PTh), and poly(3,4-ethylenedioxythiophene) (PEDOT) [81]. Their properties can be adjusted through surface functionalization and doping. The conductivity of conductive polymer originates from the conjugated double bonds in the polymer matrix, with conductivity (in oxidized and reduced states) ranging from 10^{-7}~10^{3} S·cm^{-1} [82]. Unlike adding conductive nanostructures to the matrix, conductive polymers themselves can participate in the construction of tissue engineering scaffolds [83]. Therefore, research involving conductive polymers focuses more on building conductive template networks and designing continuous conductive structures to achieve higher and more stable conductivity [84].

3.2. Piezoelectric Biomaterials

The positive role of bioelectricity in natural bone during bone development and fracture healing has been extensively studied. Piezoelectricity-mediated regulation of cellular functions includes cell proliferation, cell adhesion, and osteogenic differentiation of stem cells [7,85,86], so that it is commonly used in self-powered nanogenerators for hard tissue regeneration. The crystal structure of piezoelectric biomaterials is non-centrosymmetric. When subjected to mechanical force, the positive and negative charges inside the crystal undergo relative displacement, moving from the center in opposite directions, generating a dipole moment. This results in the accumulation of positive and negative charges on the opposite sides of the material. This inherent charge-separation capability enables piezoelectric implants to provide localized electrical stimulation without requiring external power sources; instead, they harvest biomechanical energy from physiological motions such as muscle activity, cellular traction, or daily movement, transforming transient mechanical deformations into endogenous electrical cues that support tissue repair.

This section highlights the key characteristics, applicable ranges, and research progress of major categories of piezoelectric biomaterials: inorganic piezoelectric crystals, organic piezoelectric polymers, and organic-inorganic piezoelectric composites.

3.2.1. Inorganic Piezoelectric Biomaterials

Piezoelectric ceramics represent the most widely studied class of inorganic piezoelectric biomaterials and are capable of interconverting mechanical and electrical energy. Generally, the higher the piezoelectric coefficient of piezoelectric ceramic, the better its piezoelectric performance. Perovskite and wurtzite are two kinds of most common crystal structures in piezoelectric ceramic. Perovskite belongs to the cubic crystal system and has the general formula ABO_3, including barium titanate (BTO), potassium sodium niobate (KNN), and lithium sodium potassium niobate (LKNN). BTO, the first piezoelectric biomaterial applied in bone repair, is a representative example [87]. Due to its strong electromechanical coupling capability, excellent mechanical properties, and good biocompatibility, BTO has been fabricated into structurally diverse scaffolds, including porous bulk materials for repairing bone defects and guided bone regeneration membranes consisting of BTO nanoparticles [88–90]. However, BTO suffers from poor degradability, insufficient bioactivity, and potential toxicity.

Wurtzite-structured materials, which belong to the hexagonal crystal system, exhibit both semiconducting and piezoelectric properties [91]. Zinc oxide (ZnO) is the most representative example [92]. Since the polarization direction of wurtzite cannot be altered by an electric field, these materials can only generate dipole moments when subjected to mechanical forces along specific crystal directions. Although the piezoelectric coefficients of wurtzite materials are generally lower than those of perovskites, the piezoelectric potentials they generate are comparable to cell membrane potentials, sufficient to regulate cellular behaviors [93,94].

Hydroxyapatite is the principal mineral component of bone and dentin, and its electrical properties have also attracted interest in the development of electroactive biomaterials. Lang et al. investigated synthetic nanocrystalline hydroxyapatite thin films deposited on silicon substrates and reported piezoelectric responses and electric-field-induced polarization switching consistent with ferroelectric behavior [95]. These findings concern the specific thin-film system investigated and should not be generalized to all hydroxyapatite materials or to natural bone. In particular, this study does not directly establish the contribution of hydroxyapatite to the piezoelectric response of natural bone. Such a contribution requires further evidence obtained under physiologically relevant conditions.

3.2.2. Organic Piezoelectric Polymer

Natural piezoelectric polymer, such as collagen, keratin, cellulose, chitin, and chitosan, exhibit piezoelectric coefficients of similar magnitude. For instance, collagen has a piezoelectric coefficient d_{14} of about 0.096 pC N^{-1} [96]. Additionally, the piezoelectric properties of natural polymer are closely related to their microstructure [97], pH [98], and degree of mineralization [99]. Synthetic piezoelectric polymer includes polyvinylidene fluoride (PVDF) and its copolymer poly(vinylidene fluoride-trifluoroethylene) [P(VDF-TrFE)], poly-L-lactic acid (PLLA), polyhydroxybutyrate (PHB), and polyamides [100]. Among them, PVDF exhibits a relatively high piezoelectric coefficient of 34 pC N^{-1}. PVDF and its copolymers are considered to have great potential in hard tissue repair, serving as excellent biomimetic substitutes for hard tissue [101,102]. PVDF-based piezoelectric polymer exhibits flexibility, impact resistance, ease of processing, and biocompatibility, but its piezoelectric performance is significantly weaker than that of piezoelectric ceramic. Although the piezoelectricity of piezoelectric polymer can be enhanced by stretching or poling along the direction of the piezoelectric coefficient, most single-component piezoelectric polymer struggles to reach the threshold for cell stimulation through mechanical force generated by daily activities. Consequently, piezoelectric polymers are frequently integrated with ceramics to form composite systems, which combine the advantages of both material classes and compensate for their respective limitations [103].

3.2.3. Organic-Inorganic Piezoelectric Composites

Natural bone contains a hierarchical organic-inorganic architecture in which collagen provides a structural framework and tensile resistance, while the apatite mineral phase contributes stiffness. This organization provides structural inspiration for organic-inorganic piezoelectric composites. However, the contribution of the mineral phase to the piezoelectric response of natural bone should not be inferred solely from measurements on synthetic hydroxyapatite thin films. Inorganic biomaterials possess superior mechanical properties, helping to enhance the stiffness of the material or create topological structures to increase surface roughness [104]. The incorporation of organic piezoelectric polymer helps to improve the toughness while enhancing overall biocompatibility, protecting the body from mechanical damage. Encouragingly, compared to single-component piezoelectric biomaterials, composite piezoelectric biomaterials typically show enhanced piezoelectric performances. Huang et al. applied a dynamic pressure during the manufacture of a PVDF/BTO composite with a high $g_{33} \approx 1610 \times 10^{-3}$ Vm N^{-1} [105]. In summary, organic-inorganic piezoelectric composites effectively mimic the bioelectric microenvironment of the human tissues, promoting cell adhesion, proliferation, and osteogenic differentiation, and even the mineralization of collagen fibrils. These attributes make them a highly promising class of biomaterials for bone defect repair [103,106].

The design strategies for conductive biomaterials can be summarized into two approaches: (1) Single-component conductive biomaterials forming porous conductive scaffolds through self-assembly, templating, etching, etc. (2) Multiple conductive biomaterials participating in the construction of composite biomaterials through blending, forming double-network structures, solvent exchange, etc.

Table 1. Construction methods and significant contributions of conductive biomaterials for bone tissue engineering.

Conductive Biomaterials	Conductive Components	Electrical Conductivity (S/m)	Electrical Stimulation Parameters	Other Electrical Parameters	Construction Methods	Significant Contributions of Conductive Biomaterials	Refs.
Graphene and derivatives	graphene	NR	Cyclic stimulation: ≤0.3 V, 1 Hz; 3-day study.	NR	(1)	Promote osteogenesis and neurogenesis	[107]
	graphene and GO	NR	NR	NR	(1)	Induce reactive oxygen species	[108]
	GO/nanohydroxyapatite/polydopamine	160 (10 wt‰ PGO; maximum)	Applied 300 mV, 30 min/day; 7–21 days depending on assay. Screened: 0/300/600/900 mV.	CV redox peaks: 0.38 and 0.08 V	(2)	Support cell adhesion and proliferation	[60]
	GO/PVA/chitosan	NR	NR	NR	(2)	Slow the drug release rate	[109]
	GO/quaternized chitosan/ polydopamine	NR	NR	NR	(2)	Enhance angiogenesis, reduce the inflammatory response	[110]
	rGO/gold nanodots/nanohydroxyapatite	NR	NR	NR	(2)	Improve conductivity	[111]
	rGO/tricalcium phosphate/gelatin/chitosan	NR	NR	NR	(2)	Provide mechanical resistance and stability, improve surface biomineralization, provide antibacterial property	[57]
	GOQDs/GelMA	NR	NR	NR	(2)	Regulating mitochondrial dynamics	[112]
CNTs	CNT bundles	>200 (solid CNT/ssDNA@CNT pellets; not whole-scaffold bulk conductivity)	100 mV/mm, 20 Hz, 2 h/day; carbon electrodes; ALP/OCN assessed at day 14.	NR	(1)	Improve the adhesion, proliferation, and differentiation of pre-osteoblast cells	[113]
	MWCNTs/PLLA	NR	DC 1.5 V, 1.5 h/day; days 1–7, 8–14, or 15–21; perpendicular to aligned fibers.	NR	(2)	Improve osteogenic differentiation of BMSCs	[114]
	fMWCNTs/chitosan/β-Glycerophosphate	NR	NR	NR	(2)	Improve electrical conductivity and mechanical properties	[64]
	fMWCNTs/chitosan/Fe_2O_3 and SrO_2 nanoparticles/polyurethane	NR	NR	NR	(2)	Upregulate osteogenic gene expression, improve mechanical strength	[115]
	CNTs/CMC	NR	NR	CV and EIS monitoring	(2)	Improve mechanical properties	[116]
	CNTs/PAGP	NR	Applied ES	NR	(2)	Promote cell proliferation and expressions of osteogenic markers of BMSCs	[117]
	CNTs/black phosphorus/OPF	≈0.008 (CNTpega 16 mg/mL; BP 0.8 mg/mL)	100 mV/mm, 20 Hz, 2 h/day for 21 days; carbon electrodes.	NR	(1)	Enhance mechanical strength and electrical conductivity	[118]
PPy	PPy	NR	Applied −0.8 V for 30 s to detach cell sheets (not osteogenic ES dosing).	NR	(1)	Provide conductivity and surface modifiability	[119]
	PPy/GelMA/Fe	NR	Applied 250 mV, 20 min/day	NR	(2)	Provide conductivity	[120]
	PPy/polydopamine/hydroxyapatite	NR	Applied ES reported	NR	(2)	Provide electroactivity, cell affinity, and antioxidative activity	[121]
	PPy/Dex/Ti	NR	Electrical triggering of Dex release	NR	(2)	Make drug release controllable	[122]
PANi	PANi/PLA	NR	NR	NR	(2)	Provide conductivity and promote osteogenic differentiation	[123]

Table 1. *Cont.*

Conductive Biomaterials	Conductive Components	Electrical Conductivity (S/m)	Electrical Stimulation Parameters	Other Electrical Parameters	Construction Methods	Significant Contributions of Conductive Biomaterials	Refs.
PEDOT	PEDOT:PSS/PAA	2.47×10^4	NR	NR	(2)	Form a continuous conductive network through template-directed assembly	[84]
	PEDOT/PSS/CaP/$MgTiO_3$/Alg/MAA	NR	ES reported	NR	(2)	Provide biocompatibility, conductivity, and solution processability	[124]
Metal	PATGP/PDA /AgNPs	NR	NR	NR	(2)	Provide antibacterial and conductive properties	[125]
	PCL/cellulose/AgNPs	NR	NR	Three-electrode electrochemical characterization under UV	(2)	Provide antibacterial property	[77]
	Mineralized collagen I/Ag uNWs	NR	No external excitation for scaffold-generated stimulation.	Self-generated current ≈4.0 μA in PBS; *in vivo* ≈4.5 μA at 24 h.	(2)	Promote osteoblast attachment and proliferation and inhibit bacterial activity	[74]
	MXene/RSF	≈0.04 maximum (MXene 8 mg/mL)	Applied 100 mV/mm for selected 0.4% MXene/RSF	Piezoresistive response	(2)	Provide conductivity and promote bone regeneration	[126]
	MXene/SS	NR	NR	NR	(2)	Promote osteogenic proliferation and differentiation	[44]
	$Mo_2Ti_2C_3$/TPAOH/gelatin	NR	NR	NR	(2)	Promotes osteogenesis	[127]

Table 2. Composition, electrical properties, stimulation conditions, and bone-regenerative effects of piezoelectric biomaterials.

Material or Device	Piezoelectric Coefficient d_{33} (pC/N)	Electrical Conductivity (S/m)	Generated Voltage (V; Type Specified)	Generated Current (μA; Type Specified)	Other Electrical Parameters	Bone-Related Evidence and Contributions	Reference
ZnO nanoparticle/PVDF electrospun membrane	NR	NR	NR	NR	15,000 V used for electrospinning (fabrication only)	*In Vitro* osteoblast proliferation and antibacterial tests; no verified animal defect-healing endpoint	[128]
PCL-$BaTiO_3$ scaffold (PCL-65BT)	2.6 (PCL-65BT)	NR	NR	NR	Poling: 15,000 V, 15 min (not cell stimulation)	MC3T3 preosteoblasts; ultrasound-assisted proliferation and osteogenic gene expression *in vitro*	[129]
AESO with 10 wt% Ag-TMSPM-poled $BaTiO_3$ (AESO-10ATP)	0.9	NR	NR	0.1464 (output; circuit condition NR)	NIR-triggered shape recovery; not an electrical stimulation voltage	BMSC osteogenic differentiation and *in vivo* bone-defect repair	[130]
Gelatin/PEDOT:PSS/Ca,Mn-co-doped $BaTiO_3$ (Gel-PD-CMBT)	NR	59	NR	NR	Conductivity originally 0.59 S/cm	Osteogenic differentiation *in vitro* and new-bone formation *in vivo*	[131]
$BaTiO_3$-coated Ti_6Al_4V scaffold (BT/Ti)	NR	NR	NR	NR	NR	Macrophage/osteoblast assays and bone repair; M2 polarization, MAPK/JNK inhibition and OXPHOS activation	[132]
Bio-S: CS/HAp bone layer + GelMA/alginate/PWH periosteal layer	≈9.41 (periosteal hydrogel layer only)	NR	Pending verification	Pending verification	Hydrogel: quasistatic d_{33} testing; voltage/current labels require clarification	Rat 5-mm calvarial defects; neurovascularized bone regeneration; endpoint at 8 weeks	[133]
Polarized $BaTiO_3$/TCP-derived porous scaffold with rhBMP-2 (P-BTCP)	10 (P-BTCP, before assigning a coating-dependent change)	NR	NR	NR	Poling field 6×10^6 V/m, 20 min (fabrication)	BMSCs and rat femoral defects; sustained rhBMP-2 delivery and enhanced BMPR-mediated osteogenesis	[134]
Zn-apatite/gelatin/PLLA membrane + resveratrol-loaded microsphere hydrogel (JPS)	0.9 (JPS)	NR	0.6 (device output; not confirmed Voc)	NR	PS/ZPS controls: d_{33} 1.2/1.8 pC/N; outputs 0.7/1.2 V	Diabetic mouse 3-mm calvarial defects; endothelial metabolism and H-type vascularization support bone regeneration	[135]

Table 3. Device configurations, electrical outputs, stimulation conditions, and bone-regenerative effects of triboelectric and hybrid triboelectric–piezoelectric systems.

Material or Device	Generator Voltage (V; Type Specified)	Generator Current (μA; Type Specified)	Transferred Charge (nC; Type Specified)	Power Density (mW/m^2)	Field Delivered to Cells or Tissue (V/m)	Stimulation Current (μA)	Activation and Stimulation Conditions	Bone-Related Evidence and Contributions	Reference
PTFE/Ag triboelectric + polarized PVDF piezoelectric HTP-NG; ECM/AlgMA/BP@PDA hydrogel	≈35 (Voc, hybrid; benchtop)	≈3.7 (Isc, hybrid; benchtop)	≈23 (Qsc, hybrid)	≈344.4 (instantaneous; 30 MΩ)	≈500 (*in vitro*)	≈0.08 (*in vitro*)	Bench: 1 cm^2 working area, ≈6 kPa; *in vivo* rehabilitation walking	Rat critical-sized femoral defects; conductive hydrogel plus rehabilitation-generated ES improves bone regeneration	[136]
PPCs-TENG; silk-fibroin peptide-grafted PDA/polyacrylamide electrode	NR	NR	NR	NR	NR	NR	Host motion-dependent biofeedback; quantitative protocol pending verification	BMSCs/HUVECs and critical-sized bone-defect repair *in vivo*; Piezo1/calcium mechanotransduction	[137]
Wearable pulsed TENG (WP-TENG); friction-pair details pending verification	NR	NR (device Isc)	NR	NR	NR	30 peak (optimized)	Body movement; stimulation schedule pending verification	Aged BMSCs/HUVECs and *in vivo* bone repair; Piezo1-mediated rejuvenation and angiogenesis	[138]

4. Engineering the Electro-Regenerative Microenvironment for Bone Repair

Bone repair is a highly coordinated and dynamic regenerative process rather than a simple outcome of osteogenesis alone. Following trauma, infection, or tumor resection, bone healing proceeds through a well-defined sequence that begins with antibacterial and anti-inflammatory responses and local immune activation, followed by vascular and neural ingrowth, and ultimately culminates in new bone formation and remodeling. The initial inflammatory and immune responses and local immune activation play a decisive role in shaping the regenerative microenvironment by clearing debris, preventing infection, and directing the recruitment and differentiation of reparative cells. In complex anatomical sites such as the oral and maxillofacial region, effective antibacterial control is a critical prerequisite for successful regeneration, as persistent microbial challenge can severely impair subsequent angiogenesis, neurogenesis, and osteogenesis. As healing progresses, coupled angiogenic and neurogenic processes establish vascular-neural networks that provide metabolic support, trophic cues, and regulatory signals essential for bone regeneration. Accumulating evidence highlights tightly interconnected regulatory axes, including immunomodulation, angiogenesis and osteogenesis coupling, and the neurobone axis, that collectively govern functional bone regeneration [139].

Within the ERM framework, electroactive biomaterials coordinate these biological processes through bioelectrical cues, guiding bone healing in a spatiotemporally controlled manner. Electroactive biomaterials, by virtue of their inherent electrical properties, are able to regulate cell behavior, influence bioelectrical signaling, and promote tissue regeneration. These materials exhibit notable advantages in orchestrating osteogenesis, angiogenesis, and neurogenesis, making them highly promising candidates for the treatment of bone defects. Collectively, electroactive biomaterials provide a compelling strategy to improve the efficacy of bone repair and represent an important frontier in regenerative medicine.

4.1. Antibacterial and Anti-Inflammatory Effects

For open fracture, wound infection not only hinders the healing process, leading to nonunion, but also increases the risk of deep infections, such as osteomyelitis. Bacterial infection triggers local and systemic inflammatory responses, releasing large amounts of pro-inflammatory cytokines (e.g., TNF-α, IL-1β, IL-6). These cytokines activate osteoclasts, promoting bone resorption, while simultaneously inhibiting osteoblast activity and reducing bone formation. Therefore, antibacterial property is a crucial aspect of the bone regeneration process. This section outlines three mechanisms by which antibacterial electroactive biomaterials exert their effects.

Due to the charged nature of bacterial membrane, when bacteria come into contact with a surface of opposite charge, their lipid bilayer structure is disrupted. As mentioned earlier, piezoelectric biomaterials can convert mechanical energy into electrical energy, causing different surfaces to carry opposite charges. Swain et al. demonstrated that the positively polarized surface of a hydroxyapatite-barium titanate composite disrupted bacterial membrane during cultivation, as the positive charge on the polarized surface neutralized the negative charge on the bacterial surface [140]. Another study on ZnO/PVDF composite nanofiber scaffolds also demonstrated that the piezoelectric properties of the scaffold can inhibit bacterial growth [128], promoting the formation of structurally intact new bone without inflammatory cell aggregation.

The photoelectric effect of many electroactive biomaterials induces the generation of reactive oxygen species (ROS). Some electrons leak during the respiratory chain transfer, reacting with oxygen molecules to form superoxide anions (O_2^-), which are then chemically converted into other ROS, such as hydrogen peroxide (H_2O_2) and hydroxyl radicals (·OH). In a biological context, ROS are natural byproducts of normal oxygen metabolism and play important roles in cell signaling and homeostasis. However, under environmental stress (e.g., ultraviolet light, extreme temperature, and hypoxia), ROS levels can increase dramatically, potentially causing severe damage to cell structures. This phenomenon is known as oxidative stress. Xu et al. used ultrasound to drive a PCL composite piezoelectric material (piezoPCL) containing Au-modified BTO nanoparticles, generating oxidative stress at the implant-bacteria interface. This effectively inhibited the activity of surface-attached Staphylococcus aureus by disrupting the cell membrane and depleting sugar energy (Figure 3B) [141]. After discovering the critical role of immune cells, such as macrophages, in clearing bacteria on piezoelectric surfaces, the team further investigated immune regulation, enriching the theoretical framework of antibacterial piezoelectric biomaterials [142]. Another study utilized the synergistic effects of Fe_2O_3, SrO_2 nanoparticles, and fMWCNTs to induce oxidative stress in functionalized nanoparticles, releasing ROS to kill bacteria [115].

Even without electrical stimulation, the intrinsic properties of electroactive biomaterials can achieve antibacterial effects. The sharp nanoscale edges of graphene can also function as nanoknives to disrupt bacterial membranes and lyse bacteria. Li et al. used layer-by-layer (LBL) deposition technology to alternately deposit GO

and lysozyme (Lys), creating an ultrathin GO/Lys film tens of nanometers thick. The sharp nanoscale edges of the film exhibit ultra-high bactericidal efficiency with low GO content and low cytotoxicity, but their non-specific destruction of bacterial and cell membranes may harm normal cells (Figure 3A) [143]. Sun et al. demonstrated that wireless electric stimulation (ES) modulates the immune microenvironment primarily through tuning the paracrine profile of DPSCs, which in turn drives the polarization of macrophages toward the anti-inflammatory M2 phenotype—a critical step in resolving inflammation and promoting tissue healing (Figure 3C) [144].

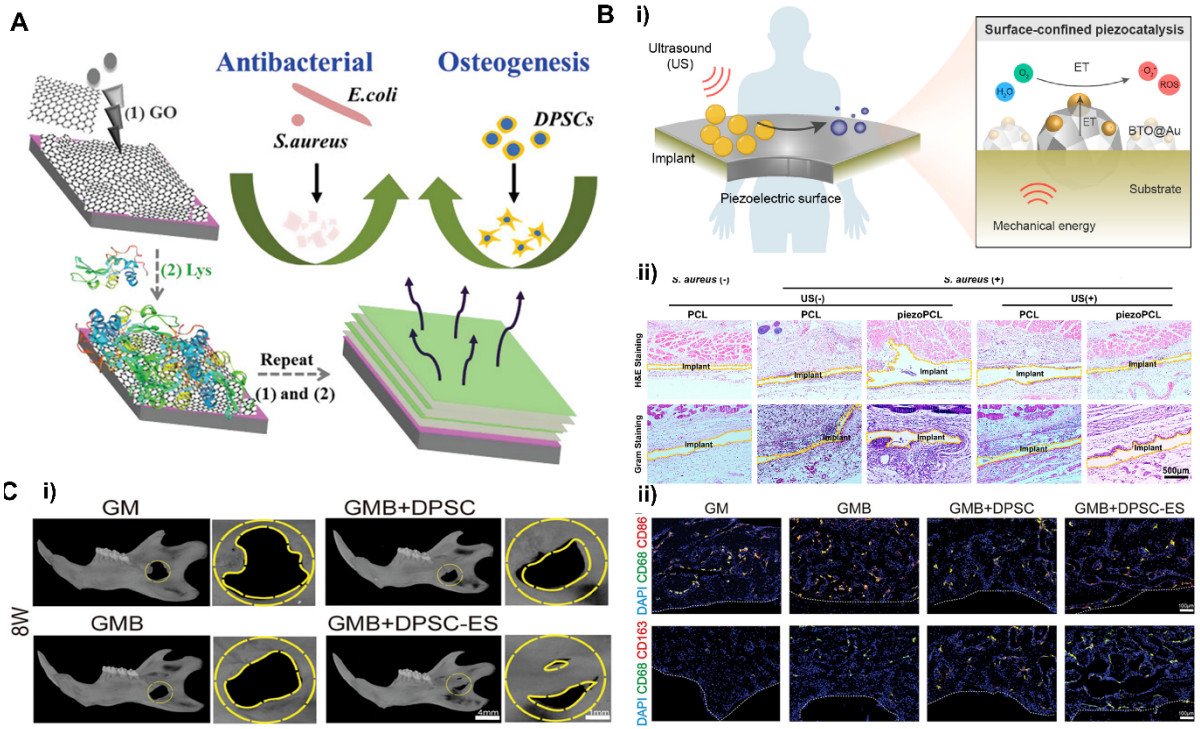


Figure 3. Electroactive biomaterials with antibacterial and anti-inflammatory effects for bone repair and regeneration. (**A**) Schematic diagram of the fabrication of $(GO/Lys)_n$ and its basic functions. Reproduced from Ref. [143] with permission of American Chemical Society, © 2019. (**B**) (**i**) The proposed antibacterial mechanism by surface-confined piezocatalytic ROS production from metal/piezoelectric nanocomposite-embedded implant. ET: electron transfer. (**ii**) H&E and Gram staining images after 1 day of treatment with different samples. Implant position is marked with a yellow dashed line. Reproduced from Ref. [141] with permission of American Chemical Society, © 2023. (**C**) (**i**) Micro-CT images of mandibular bone defects 8 weeks after microsphere hydrogel implantation. (**ii**) Immunofluorescent staining of $CD68^+$ $CD86^+$ macrophages, $CD68^+$ $CD206^+$ macrophages protein of sections from each group at the first week postoperatively. Reproduced from Ref. [144] with permission of Wiley-VCH, © 2023.

4.2. Immunomodulation

Many diseases cause bone loss through inflammation, involving the recruitment of macrophages and other inflammatory cells to bone defects [145]. Studies have shown that various immune cells, particularly macrophages, can secrete relevant cytokines, directly affecting the immune response and regenerative repair of bone. Macrophages have two phenotypes: M1 and M2. M1 macrophages can secrete various pro-inflammatory cytokines, such as TNF-α, IL-1β, and IL-6, which recruit and activate other immune cells, thereby enhancing the inflammatory response. However, excessive inflammation may lead to tissue damage. M2 macrophages can secrete various growth factors, extracellular matrix components, and anti-inflammatory cytokines, such as TGF-β, IGF-1, and IL-10. These substances not only promote cell proliferation, angiogenesis, and tissue remodeling but also suppress excessive inflammatory responses, preventing tissue over-damage [146]. Electroactive biological scaffolds and self-powered systems can both achieve immunomodulatory effects. Electrical stimulation significantly enhances macrophage phagocytosis and uptake, selectively regulates cytokine production, and promotes the transition of macrophages from the pro-inflammatory M1 phenotype to the pro-healing M2 phenotype [147,148], positively impacting anti-inflammation and thereby promoting bone healing [142].

Li et al. fabricated a conductive alginate/gelatin (AG) scaffold doped with polydopamine-mediated graphene oxide (PGO) and nano-hydroxyapatite (PHA), which exhibits excellent conductivity, mechanical properties, and liquid absorption capacity. The scaffold is biodegradable, making it suitable for long-term implantation. The

scaffold was shown to promote the transition of macrophages from the M1 to the M2 phenotype, accompanied by a reduction in pro-inflammatory cytokine levels, thereby enabling local immunomodulation under diabetic conditions and promoting periodontal bone regeneration. Mechanistic studies further suggested the involvement of the RhoA/ROCK signaling pathway (Figure 4A) [60]. Dutta et al. developed a highly stable and conductive bioink based on polypyrrole-grafted gelatin methacryloyl (GelMA-PPy). A triple-crosslinking (thermal-photo-ionic) strategy was employed to fabricate a hydrogel with a dynamic semi-interpenetrating polymer network (semi-IPN), exhibiting excellent shear-thinning properties and improving shape fidelity and structural stability during 3D printing. Results showed that the scaffold could respond to external electrical stimulation, enhancing the osteogenic differentiation of BMSCs, attributed to the promotion of M1-to-M2 macrophage transition by electrical signals and the regulation of NOTCH/MAPK/SMAD signaling and the Wnt/β-catenin pathway (Figure 4B) [120]. However, electrical stimulation does not invariably promote M2 polarization. Kong et al. reported that localized electrical stimulation generated by ultrasound-driven piezoelectric β-PVDF films enhanced pro-inflammatory M1 macrophage polarization by promoting Ca^{2+} influx through voltage-gated calcium channels and activating the Ca^{2+}-CAMK2A-NF-κB signaling axis [149]. This study investigated macrophage regulation in the context of tumor immunotherapy and should not be interpreted as direct evidence of a pro-regenerative immune response in bone repair. It highlights the need to evaluate the direction of macrophage polarization under the specific material and stimulation conditions employed.

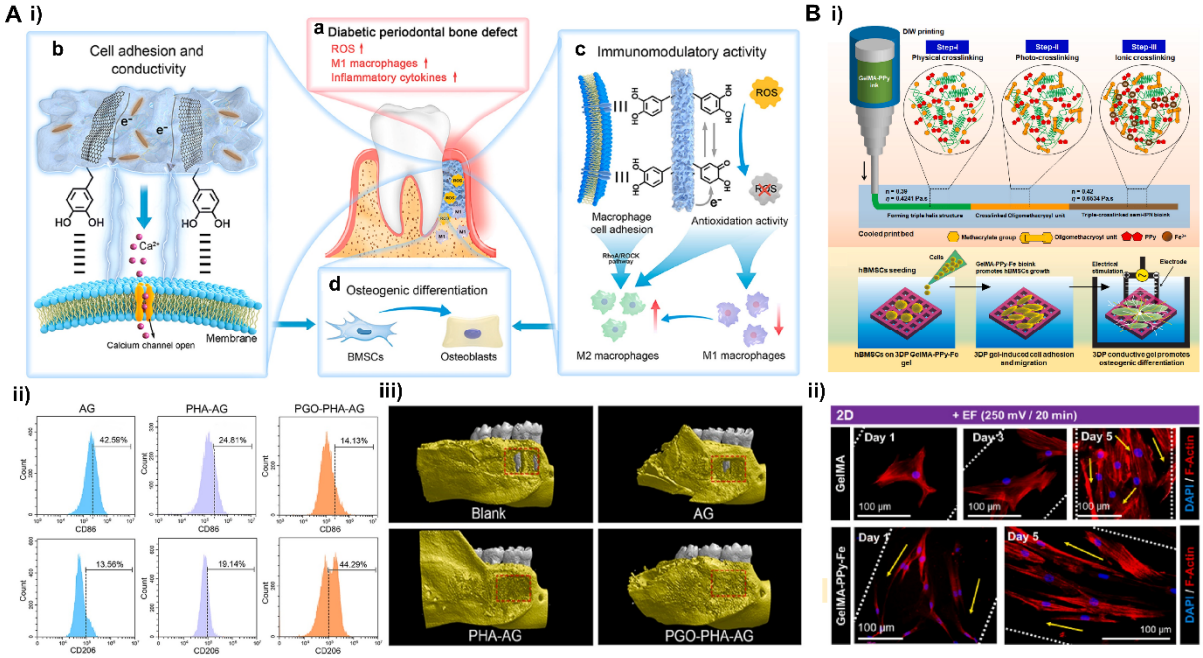


Figure 4. Electroactive biomaterials modulating osteoimmunology for bone repair and regeneration. (**A**) (**i**) (**a**) ROS, M1 macrophages, and inflammatory cytokines are overexpressed in the local diabetic periodontal microenvironment. (**b**) The scaffold promoted cell adhesion and transferred the endogenous electrical signals to cells, activating Ca^{2+} channels. (**c**) The cell adhesion and ROS-scavenging properties of the PDA conferred the scaffold with an immunomodulatory activity that reduced M1 macrophage polarization and activated M2 macrophages that secreted osteogenesis-related cytokines. (**d**) The conductivity and immunomodulatory activity synergistically promoted periodontal bone regeneration. (**ii**) Polarization of macrophages was evaluated by expression of CD86 (M1) and CD206 (M2) using flow cytometry. (**iii**) Micro-CT images of the rat mandible at the site of implantation. Reproduced from Ref. [60] with permission of Elsevier, © 2022. (**B**) (**i**) Schematic illustration for the fabrication process of 3D printed triple-crosslinked (thermo-photo-ionic crosslinking) GelMA-PPy based hydrogel for improving the conductivity and bioactivity and an overview of direct current stimulation for regulating stem cell proliferation and osteogenic differentiation. The n and η represents the shear-thinning index and apparent viscosities of the GelMA and GelMA-PPy-Fe bioink, respectively. (**ii**) Immunofluorescence staining showing the orientation of F-actin (red) and nucleus (blue). Reproduced from Ref. [120] with permission of Elsevier, © 2023.

4.3. Angiogenesis

Angiogenesis is one of the key factors in bone repair. Insufficient vascularization can cause nonunion and ischemic necrosis, increasing the risk of bone repair failure. Thus, enhancing the angiogenic capacity of bone

implants is clinically important [150]. Wang et al. transplanted mitochondria from human bone marrow mesenchymal stem cells (BMSCs) into BMSCs of the same batch and passage number. They found that the transplanted mitochondria significantly enhanced the ability of co-transplanted BMSC-endothelial cells to promote angiogenesis, facilitated the formation of functional vascular networks in rat cranial defects through the DLL4-Notch1 signaling pathway, and improved bone repair outcomes, further confirming the importance of angiogenesis in bone repair [151]. Therefore, vascular regeneration not only facilitates the delivery of oxygen, nutrients, and regenerative cells but also contributes to the establishment of a supportive microenvironment for bone repair. Within the ERM framework, bioelectrical cues mediated by electroactive biomaterials may further promote angiogenesis and its coupling with osteogenesis.

The electroactive hydrogel prepared from MXene and regenerated silk fibroin (RSF) exhibits excellent capabilities in promoting HUVEC migration and vascular formation under an electric field stimulation of 100 mV/mm. After implanting it into cranial defects for 12 weeks, researchers performed 3D reconstruction of the newly formed blood vessels, showing that the material formed a very dense vascular network under electrical stimulation. Mechanistic study indicates that electrical stimulation promotes direct osteogenesis by activating the Ca^{2+}/CALM signaling pathway, while also stimulating the regeneration and migration of endothelial cells, accelerating angiogenesis, and thereby promoting indirect osteogenesis (Figure 5A) [126]. Wang et al. prepared a conductive hydrogel using dopamine-modified black phosphorus and methacrylated sodium alginate, contributing to the construction of a hybrid piezoelectric/triboelectric nanogenerator (HTP-NG). By capturing energy generated during patient-initiated or passive functional exercises, it produces biphasic electrical pulse signals in response to rehabilitation movements. *In Vivo* experiments showed that the conductive hydrogel implanted with the HTP-NG system significantly promoted angiogenesis, thereby supporting bone regeneration [136]. Fan et al. designed a three-dimensional semiconductor heterojunction network (3D-NTBH) implant based on titanium dioxide nanowires and bismuth oxide nanodots. By mimicking the perivascular microenvironment of bone tissue, it regulates the energy metabolism of endothelial cells (accelerating glycolysis), thereby driving angiogenesis and osseointegration, and providing a new direction for the vascularization design of bone implants (Figure 5B) [152].

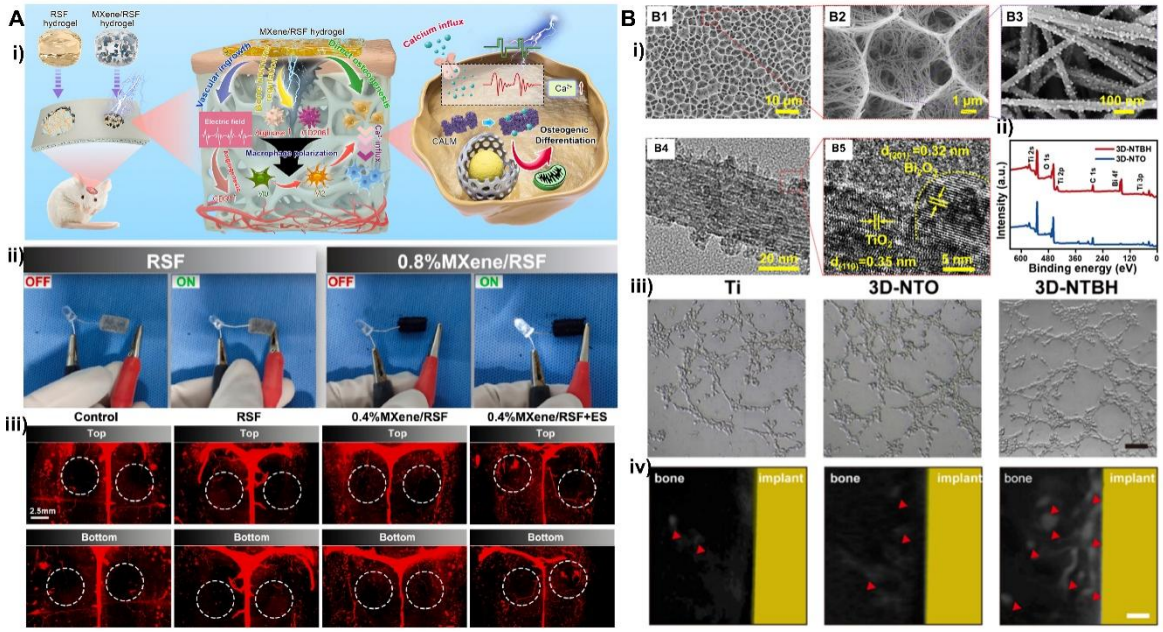


Figure 5. Electroactive biomaterials promoting angiogenesis for bone repair and regeneration. (**A**) (**i**) Conceptual and effective mechanisms of the electroactive MXene/RSF hydrogels to re-establish the electrical microenvironment for bone regeneration. (**ii**) Electrically conductive pathways made of RSF and MXene/RSF hydrogels to illuminate an LED. (**iii**) Representative images of 3D reconstruction of the blood vessels at 12 weeks post-implantation. Reproduced from Ref. [126] with permission of Elsevier, © 2023. (**B**) (**i**) Surface morphologies of 3D-NTBH at different multiplicities determined by SEM. TEM images (**B4**) and HRTEM images (**B5**) of the TiO_2/Bi_2O_3 heterojunction. (**ii**) XPS spectra of 3D-NTO and 3D-NTBH for the full survey. (**iii**) Fluorescence imaging of HUVECs tube formation in 3D NTBH and control groups (scale bar: 100 μm). (**iv**) Vascular regeneration situation around implants in Ti, 3D-NTO, and 3D NTBH groups in week 2 (scale bar: 500 μm). Reproduced from Ref. [152] with permission of American Chemical Society, © 2024.

4.4. Neurogenesis

The neural network, alongside the vascular network, plays a crucial role in bone tissue engineering [153]. Dense neural and vascular networks run parallel through Haversian canals and Volkmann's canals in cortical bone, entering the bone marrow cavity to regulate bone homeostasis. Nerves can mediate the bone's response to external stimuli and secrete various neurotransmitters (e.g., CGRP, SP) and neurotrophic factors (e.g., NGF, BDNF, and GDNF), actively participating in the bone damage repair process. Therefore, it is crucial to develop bone tissue engineering scaffolds that mimic the complex structure of bone and possess neuro/vascular regulatory functions.

In recent years, numerous studies on electrical stimulation for nerve regeneration have emerged [154–157]. Electrical stimulation can induce stem cell differentiation into neurons, repair or replace damaged or lost neurons, and promote the recovery of functions impaired by nerve injury or neuropathy. Wang et al. developed a $Mo_2Ti_2C_3$ MXene-based hydrogel that facilitates neurogenesis factors nerve growth factor (NGF) and brain-derived neurotrophic factor (BDNF) expression, and aids newly born neuron marker Tuj-1 and sensory neuron marker serotonin (5-HT) and osteogenesis pathway proteins, runt-related transcription factor 2 (Runx2), osteocalcin (OCN), SMAD family member 4 (SMAD4), and bone morphogenetic protein-2 (BMP2) in the bone defect repair process, accelerating the bone defect repair process [127]. A conductive biomimetic periosteum (PD@BP) coupled with an endogenous electric field and black phosphorus (BP) was constructed in another study. It regulates the transformation of Schwann cells into a repair phenotype through the Fanconi anemia signaling pathway, enhances the function of sensory neurons, and ultimately promotes the osteogenic differentiation of bone marrow mesenchymal stem cells (BMSCs) via nerve mediation. This provides a novel "nerve-electrical signal-osteogenesis" synergistic strategy for bone defect repair (Figure 6A) [158].

Electroactive biomaterials offer a promising strategy to couple neural regeneration with bone repair. Qin et al. reported an endogenous electric field–responsive conductive hydrogel that modulated the peri-implant microenvironment to promote nerve–bone crosstalk. The electroconductive matrix enhanced neurite outgrowth by increasing intracellular Ca^{2+} levels and activating PI3K–AKT and MEK–ERK signaling pathways. Regenerated sensory nerves subsequently released neuropeptides such as calcitonin gene-related peptide and substance P, which significantly stimulated osteogenic differentiation and bone formation. *In Vivo*, impaired sensory innervation markedly reduced osseointegration, underscoring the critical role of nerve-mediated regulation. This study highlights electroactive biomaterials as effective platforms for neural-assisted bone regeneration and functional implant integration (Figure 6B) [159].

In addition to the traditional design strategies for electroactive biomaterials mentioned above, some innovative materials have opened new avenues for researchers in the field of bone repair. A bone repair material located away from the lesion area applies electrical stimulation to the dorsal root ganglia (DRGs), triggering calcium ion influx and activating the Ca^{2+}/CaMKII/CREB signaling cascade, which leads to the transcription of calcitonin gene-related peptide (CGRP). After being synthesized in the DRGs, CGRP is transported to peripheral nerve terminals and released upon electrical stimulation (ES)-induced depolarization. The released CGRP and the subsequent increase in H-type vessel formation can promote the healing of osteoporotic fractures. Unlike material implantation at the bone defect site, this approach of utilizing *in vivo* signal transduction and active factor release for distal material implantation represents an efficient strategy for promoting bone regeneration (Figure 6C) [160]. It is undeniable that nerve regeneration facilitates the transmission of bone regeneration-related signals, and signaling pathways associated with stem cell adhesion, migration, proliferation, and osteogenic differentiation also rely on nerve regeneration. Therefore, the construction of a well-developed neural network in the bone defect area is expected to provide new strategies for the application of electroactive biomaterials in bone repair.

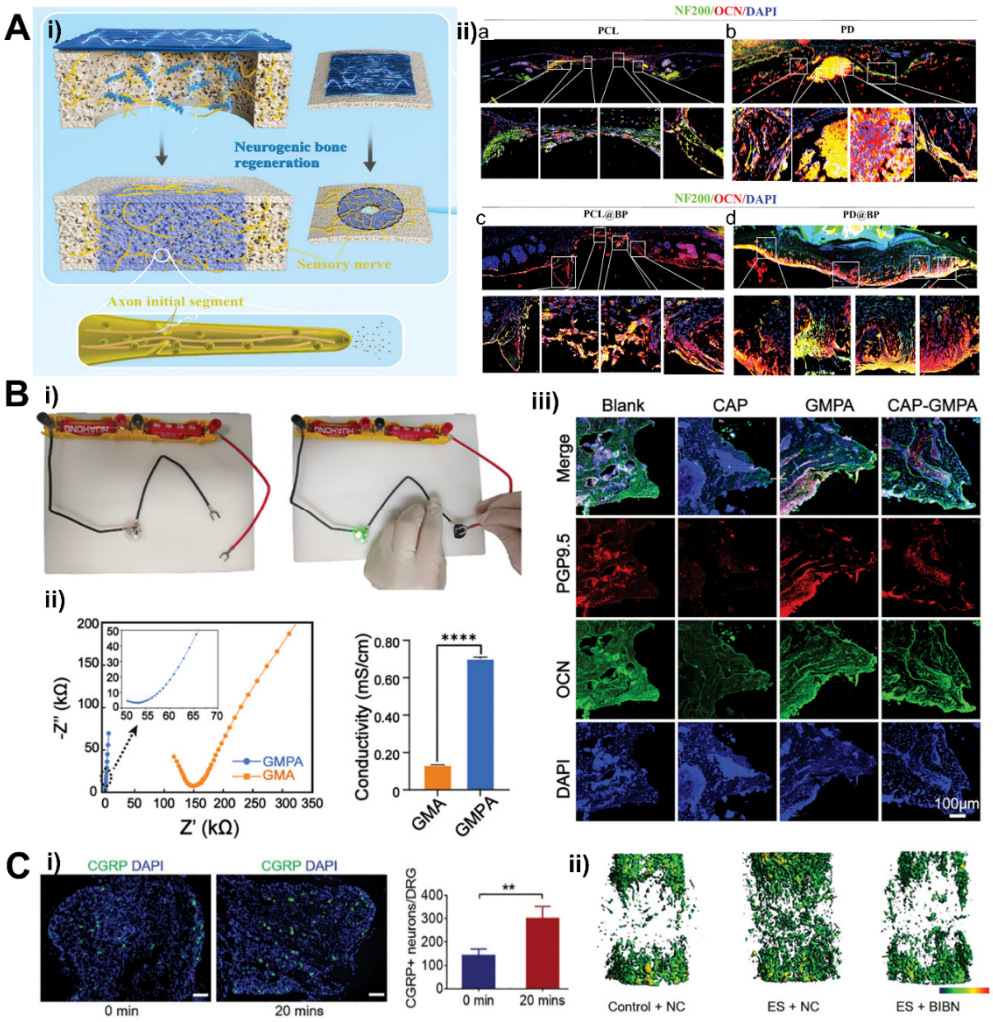


Figure 6. Electroactive biomaterials promoting neurogenesis for bone repair and regeneration. (**A**) (**i**) Schematic diagram of the PD@BP promoting neurogenic bone regeneration. (**ii**) Immunofluorescence of skull defect area, **a**–**d** indicate different groups. Reproduced from Ref. [158] with permission of Wiley-VCH, © 2023. (**B**) (**i**) Integrated circuit conductivity of the conductive GMPA hydrogel. (**ii**) Nyquist curves tested by the electrochemical workstation to demonstrate the conductivity of hydrogel. Conductivity tested by the four-point probe (n = 3, **** $p < 0.0001$). (**iii**) Immunofluorescence images of OCN and PGP9.5. Reproduced from Ref. [159] with permission of Wiley-VCH, © 2024. (**C**) (**i**) Representative images and quantification of CGRP positive neurons in DRGs at 0 and 20 min after ES (mean ± SD, unpaired Student's *t*-test, ** $p < 0.01$, n = 4 per group) (Scale bar: 50 μm). (**ii**) Representative 3D reconstructed images of the newly formed vessel around fracture line at week 2. Reproduced from Ref. [160] with permission of Wiley-VCH, © 2021.

4.5. Osteogenesis

4.5.1. Conductive Biomaterials in Bone Repair

Conductive osteogenic materials can respond to exogenous electrical stimuli, acting as intermediaries for exogenous electrical signals to regulate cell behavior and determine cell fate, while also transmitting electrical signals generated by endogenous electric fields. BP and MXene are both novel conductive osteogenic biomaterials. BP is considered as substitute for graphene and exhibits superior electromechanical properties, thermoelectricity and topological characteristic. Jing et al. incorporated Mg-modified black phosphorus nanosheets (BP@Mg) into gelatin methacrylate (GelMA). The resulting composite hydrogel was reported to improve Schwann cell migration and secretory activity, promote neuronal growth, and enhance innervated bone regeneration (Figure 7A) [161]. These outcomes should be interpreted as effects of the composite system, to which electrical cues, bioactive ion release, and other material properties may contribute. The presence of conductivity alongside improved regeneration does not, by itself, establish the independent contribution of conductivity or demonstrate synergy between electrical and ionic effects. MXene and its derivatives feature adjustable size, large surface area,

hydrophilicity, photothermal conversion, metallic conductivity, photoluminescence, near-infrared absorption, X-ray attenuation, drug-loading capacity, biocompatibility, and high conductivity. Compared to GO, the MXene family is highly diverse and demonstrates excellent hydrophilicity and stability under physiological conditions [73,162]. Fu et al. added ultra-long hydroxyapatite nanowires (UHAPNWs) at different ratios to a homogeneous MXene suspension and obtained a self-standing nanocomposite membrane through vacuum filtration. This membrane promoted cell adhesion, proliferation, and osteogenic differentiation, exhibiting outstanding mechanical properties, biocompatibility, and osteoconductivity *in vivo* at the optimal ratio (10 wt% UHAPNWs) (Figure 7B) [163]. Through roll-to-roll-assisted blade coating (RBC) integrated with sequential bridging, Wan et al. successfully fabricated scalable and high-performance $Ti_3C_2T_x$ MXene films (S-SBM). These films exhibit excellent performance in mechanical properties, electromagnetic shielding, photothermal conversion, and osteogenic regeneration, laying a foundation for the practical applications of MXene. It also provides possibilities for conductive MXene to promote osteogenesis (Figure 7C) [44].

Electroactive biomaterials have shown significant potential in enhancing bone regeneration by converting mechanical cues into bioelectrical signals. Liu et al. developed a biodegradable piezoelectric–conductive integrated hydrogel scaffold that mimics the native electromechanical microenvironment of bone. Under physiological joint motion, the scaffold generated endogenous electrical stimulation, which promoted mesenchymal stem cell migration and osteogenic differentiation through Ca^{2+}-related signaling pathways. *In Vivo* studies in large-animal osteochondral defect models demonstrated enhanced subchondral bone formation, increased trabecular thickness, and improved bone volume fraction. This work highlights how electroactive scaffolds can harness biomechanical energy to drive osteogenesis and achieve effective functional bone repair (Figure 7D) [81].

A key limitation in interpreting these composite systems is the difficulty of separating electrical effects from other material-mediated contributions. Ion release, photothermal effects under irradiation, mineral components, and changes in mechanical or surface properties may also influence osteogenesis. Accordingly, improved osteogenic outcomes in a conductive composite do not alone establish a causal relationship between conductivity and bone regeneration. Where the controls in the original studies do not isolate these factors, the reported outcomes should be attributed to the composite system as a whole, and the independent or synergistic contributions of its electrical properties remain unresolved. Further studies using appropriately matched controls are needed to distinguish these contributions.

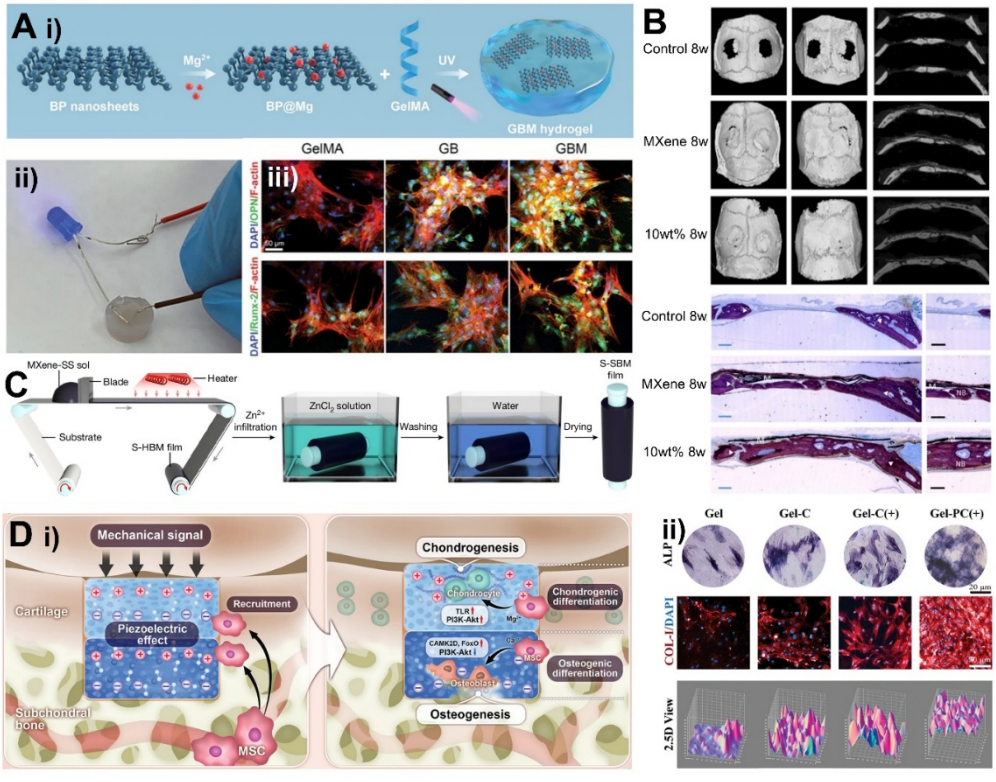


Figure 7. Representative conductive biomaterials for bone repair and regeneration. (**A**) (**i**) Schematic diagram showing construction method of GelMA-BP@Mg (GBM) hydrogel for antibacterial and innerved bone regeneration of infected bone defects. (**ii**) GBM hydrogel illuminating an LED. (**iii**) Images of OPN and Runx-2

immunofluorescence staining in BMSCs cultured on the three types of hydrogels. Reproduced from Ref. [161] with permission of Wiley-VCH, © 2022. (**B**) Reconstructed micro-CT images and Van Gieson's staining images of bone defects in control group, MXene group and UHAPNWs/MXene group at 8 weeks after surgery. Reproduced from Ref. [163] with permission of Elsevier, © 2020. (**C**) MXene-SS sol was continuously assembled into a S-HBM film, followed by Zn^{2+} infiltration to obtain an S-SBM film. Reproduced from Ref. [44] with permission of Nature, © 2024. (**D**) (**i**) Schematic diagram of biodegradable piezoelectric-conductive scaffolds for repair and reconstruction of osteochondral defects. (**ii**) ALP staining and immunofluorescence images of COL-I, along with a 2.5D view of immunofluorescence in the Gel, Gel-C, Gel-C (+), and Gel-PC (+) groups. Reproduced from Ref. [81] with permission of Wiley-VCH, © 2024.

4.5.2. Piezoelectric Biomaterials in Bone Repair

Inspired by the piezoelectric properties of bone, designing piezoelectric devices is a promising biomimetic strategy for bone regeneration. The piezoelectric nanogenerator (PENG) is a micro-generator that utilizes the piezoelectric and semiconductor properties of piezoelectric nanomaterials to convert mechanical energy from bending or compression into electrical energy. Its external stimulation methods include: cellular traction force, constant cyclic stress, ultrasound, and magnetostriction [164].

The effects of surface polarity depend on the material, cell type, and measured outcome. Dubey et al. reported enhanced cell growth on negatively charged HA-$BaTiO_3$ composites [165], while Zhang et al. demonstrated improved BM-MSC osteogenic differentiation using negative-potential $BaTiO_3$/P(VDF-TrFE) membranes (Figure 8A) [90]. On polarized P(VDF-TrFE) Janus membranes, Lai et al. found that the negative surface favored rat BMSC osteogenic differentiation, whereas the positive surface promoted human gingival fibroblast migration (Figure 8B) [89]. By comparison, Li et al. reported enhanced rat BMSC osteogenic differentiation on positively charged $LiNbO_3$ crystals [166]. These findings are not directly comparable because the substrates, polarization characteristics, and experimental protocols differ. In particular, osteogenic induction and migration assays assess distinct responses under different culture conditions. Surface potential should also be distinguished from surface charge density; without comparable charge-density measurements, polarity alone cannot explain the differences. Thus, these studies indicate context-dependent responses rather than a universal preference for positive or negative surfaces.

Therefore, researchers have combined piezoelectric ceramics and polymers with other materials or loaded them with drugs, active factors, and bioactive proteins to diversify the functionality of composite biomaterials and enhance osteogenic effects. Li et al. incorporated Ag-TMSPM-pBT (ATP) piezoelectric nanoparticles into a shape memory polymer (SMP), acrylated epoxidized soybean oil (AESO), and fabricated an AESO-ATP piezoelectric scaffold using digital light processing (DLP) 3D printing technology. This approach overcame the adverse effects of the phase difference, achieving a piezoelectric coefficient (d_{33}) of 0.9 pC N^{-1} and an output current of 146.4 nA, which is close to the piezoelectric coefficient of natural bone tissue. Notably, under near-infrared light irradiation, the AESO-ATP piezoelectric scaffold can recover its original shape, facilitating minimally invasive implantation, defect occupation, and personalized adaptation of the material (Figure 8C) [130]. A periosteum–bone inspired hierarchical scaffold with endogenous piezoelectricity also significantly promoted osteogenesis by activating mechano-electrical signaling under low-intensity pulsed ultrasound, leading to enhanced Runx2 expression, mineral deposition, and mature bone formation *in vivo* (Figure 8D) [133].

However, both piezoelectric and conductive scaffolds have limitations. Conductive biomaterials can transmit bioelectrical signals and simulate the microcurrent environment of bone tissue, but they require an external electric field, which complicates implantation application. After polarization, the charges generated by piezoelectric biomaterials are confined to their surfaces, but the widespread microcurrents in bone tissue result in limited compatibility between them. Therefore, Zheng et al. designed an electroactive scaffold by incorporating Ca^{2+} and Mn^{4+} co-modified BTO into the conductive polymer PEDOT: PSS, integrating the advantages of conductive and piezoelectric biomaterials to closely mimic the electroactive microenvironment of natural bone. Experimental results showed that the presence of the conductive matrix amplified the osteogenic promotion effect of piezoelectric nanofibers [131].

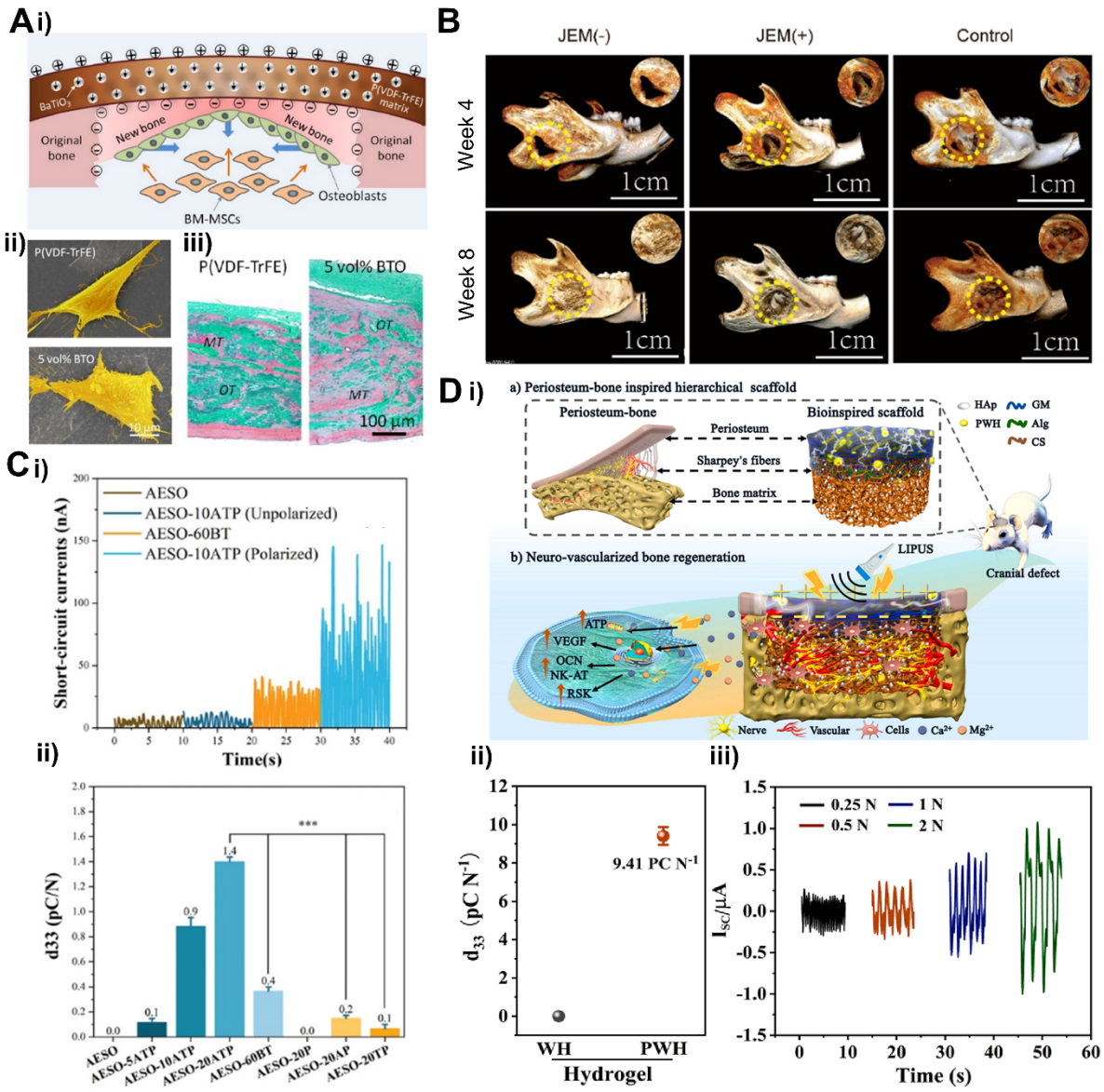


Figure 8. Representative piezoelectric biomaterials for bone repair and regeneration. (**A**) (**i**) Illustration of biomimetic electric microenvironment created by BTO NP/P (VDF-TrFE) composite membranes encouraging bone defect repair. (**ii**) Representative SEM images of cell spreading of BM-MSCs cultured for 24 h. (**iii**) Masson's trichrome staining of histological sections at 12 weeks after implantation. Reproduced from Ref. [90] with permission of American Chemical Society, © 2016. (**B**) Reconstructed micro-CT images of critical-sized rat mandibular defects at 4 and 8 weeks of JEM membrane implantation. Yellow dotted lines denote the original bone defect. Reproduced from Ref. [89] with permission of Elsevier, © 2022. (**C**) (**i**) Short-circuit currents of different scaffolds. (**ii**) Piezoelectric constant (d_{33}) of different scaffolds (n = 6). The quantitative data were expressed as mean ± SD deviation. (*** $p < 0.001$). Reproduced from Ref. [130] with permission of Wiley-VCH, © 2023. (**D**) (**i**) Schematic of a bioinspired scaffold with endogenous piezoelectricity for bone defect repair. (**ii**) Piezoelectric coefficient (d_{33}) of the GM/Alg/WH and GM/Alg/PWH hydrogels. (**iii**) Current changes in the GM/Alg/PWH hydrogel system under different force stimulation (frequency: 1 Hz). Reproduced from Ref. [133] with permission of Elsevier, © 2025.

4.5.3. Triboelectric Materials in Bone Repair

In addition to conductive and piezoelectric biomaterials, triboelectric systems represent another important approach to generating electrical cues for bone regeneration. Unlike piezoelectric materials, which rely on electromechanical coupling, triboelectric nanogenerators (TENGs) typically operate through the coupling of contact electrification and electrostatic induction. These systems can harvest mechanical energy from physiological movements or externally applied mechanical stimuli and convert it into electrical outputs for localized stimulation.

The triboelectric effect is mainly based on the coupling of contact electrification and electrostatic induction between the surfaces of two different materials. The generation of electrostatic charges when the two objects come into contact is the source of electrification for the triboelectric nanogenerator (TENG), while electrostatic induction provides the driving force to drive induced charges to flow through an external circuit, thereby generating an electric current. The alternating current triboelectric nanogenerator (AC-TENG) based on solid dielectrics is the most common device for harvesting contact electrification charges. The four basic working modes of AC-TENG are: (1) contact separation mode; (2) lateral sliding mode; (3) freestanding mode; (4) single electrode mode (Figure 9A) [12].

In recent years, implantable TENGs have become a research hotspot in osteogenic materials. Here, we mainly introduce the classic model, which primarily consists of a TENG that generates electrical stimulation and a dressing electrode that directly applies electrical stimulation to the bone defect site. Unlike batteries, TENGs, with their advantages of being lightweight, soft, stretchable, biodegradable, biocompatible, and capable of providing electrical stimulation at a threshold without being excessive, significantly reduce the occurrence of inflammation and necrosis [13], making them the ideal choice for providing self-powered medical interventions for organisms. Li et al. constructed an *in vitro* device with a pulsed planar sliding TENG connected to a cell culture dish. Combining cell and animal experiments with mechanistic studies, they proposed that triboelectric stimulation could enhance the proliferation capacity of senescent BMSCs and improve their differentiation ability (Figure 9B) [167], Further research by the group revealed that senescent BMSCs could regain vitality through the mechanosensitive ion channel Piezo1 under triboelectric stimulation. This proposed signaling mechanism enriches the theoretical framework of triboelectric stimulation in restoring stem cell vitality and promoting bone regeneration [138]. Tian et al. fabricated a flexible implantable TENG composed of a TENG with gold and aluminum electrodes to provide electrical stimulation for enhancing osteoblast function. *In Vitro* studies with the MC3T3-E1 cell line showed that electric field stimulation improved the efficiency of adherent cells by 44.68%, 72.76%, and 22.22% at 1, 3, and 6 h, respectively, compared to the control group (Figure 9C). Additionally, after 60 min' exposure in electric field, intracellular calcium ion levels increased, highlighting its improvement in osteoblast function [168].

Yao et al. developed a self-powered implantable bioabsorbable device that directly applies biofeedback electrical stimulation for fracture treatment. The electrical stimulation signals are entirely generated by joint motion, providing closed-loop biofeedback therapy that promotes rapid fracture healing. The researchers demonstrated the operation of the device in rats, achieving effective fracture healing in just 6 weeks, compared to over 10 weeks for the control group. Additionally, the experimental group showed significant increase in mineral density and bending strength by 27% and 83%, respectively, proving that electrical stimulation greatly enhances the speed and effectiveness of fracture healing (Figure 9D) [169]. However, the installation, maintenance, and long-term implantation of implantable devices increase the risk of infection. Xiao et al. constructed an ultrasound-driven, biodegradable, injectable TENG to circumvent these risks. The stable output of the device is driven by ultrasound (20 kHz, 1 W cm^{-2}), with a voltage of 356.8 mV and a current of 1.02 μA *in vivo*, and an electric field of ~0.92 V mm^{-1} *in vitro*. Cell scratch and proliferation assays showed that the delivered electrical stimulation effectively promoted fibroblast migration and proliferation. This study did not explore the impact of the injectable device on osteogenesis, but its micro-nano structural design can serve as a reference [170].

Stable and sustainable current output, real-time current monitoring, on-site data processing and regulation, and feasible fixation methods for implantable biomaterials are critical areas requiring optimization for TENGs in bone repair [13]. In the fields of supercapacitors, sensors, electronic skin, human-machine interaction, and other multifunctional soft electronic devices, TENGs have already demonstrated important characteristics such as precise sensing, controllable current output, and strong adhesion [171–173]. Based on this, implantable TENGs are expected to integrate these advantages, achieve functional optimization, and become multifunctional, highly effective, and intelligent bone repair materials.

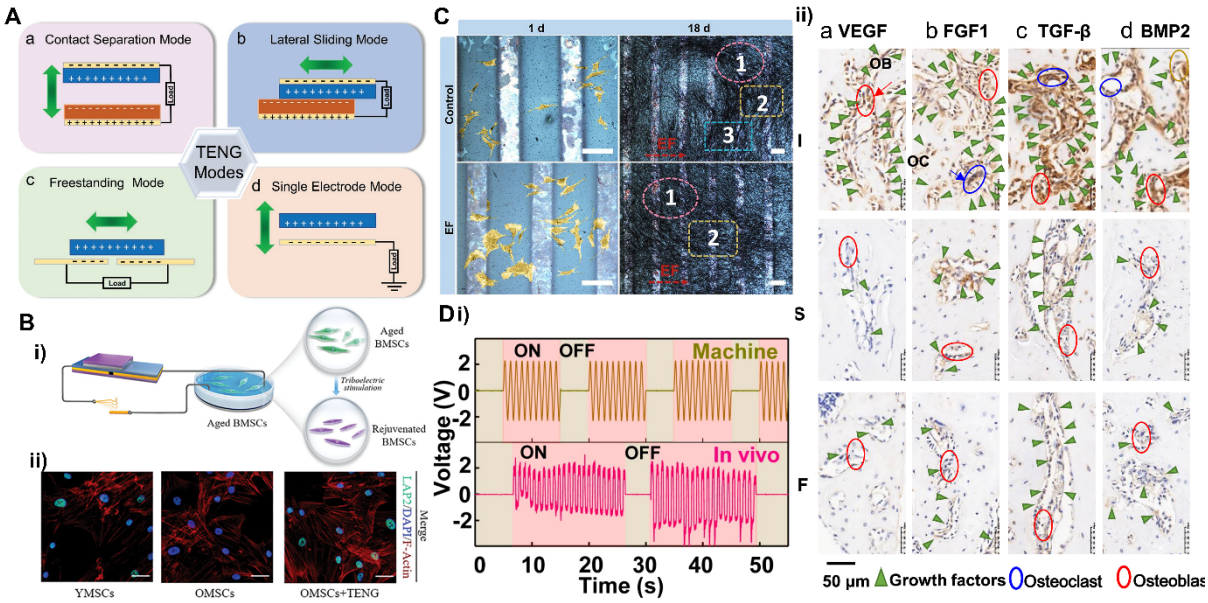


Figure 9. Representative triboelectric biomaterials for bone repair and regeneration. (**A**) Basic modes of TENG under the influence of external mechanical force. The green arrows represent the direction of motions. Reproduced from Ref. [12] with permission of Wiley-VCH, © 2023. (**B**) (**i**) Schematic illustration of rejuvenation of aged BMSCs by triboelectric stimulation with P-TENG. (**ii**) Immunofluorescence staining of LAP2 (green), nucleus (blue), and F-actin (red) (scale bar: 20 μm). Reproduced from Ref. [167] with permission of Wiley-VCH, © 2021. (**C**) ALP level implied by BCIP/NBT staining (grayish black) after stimulated for 1 and 18 days. The numbered regions outlined in pink (1), yellow (2), and cyan (3) indicate selected areas corresponding to the magnified images in Figure 4b of the original study; these magnified images are not reproduced here. Reproduced from Ref. [168] with permission of Elsevier, © 2019. (**D**) (**i**) Voltage output recorded from the FED driven by a mechanical linear motor (**Top**) and on a rat *in vivo* (**Bottom**), respectively. (**ii**) IHC staining images (10× and 40×) of multiple growth factors including VEGF (**a**), FGF1 (**b**), TGF-β (**c**), and BMP2 (**d**). Reproduced from Ref. [169] with permission of PNAS, © 2021.

5. Development Directions of Electroactive Biomaterials for Bone Repair and Regeneration

5.1. Integration of High Mechanical Strength with High Conductivity

Robust conductive scaffolds composed of electroactive biomaterials with high mechanical strength, such as GO, CNTs, and piezoelectric ceramics, possess the unique ability to trigger mechanical responses in organisms and promote bone repair and regeneration [107,113]. When conductive polymers are not involved, most studies optimize mechanical and conductive properties by controlling the ratio of conductive fillers to the polymer matrix [174,175]. However, when conductive polymers are selected to enhance biocompatibility, a trade-off between conductivity and mechanical performance often arises [176]. Excessive conductive polymer content may result in materials with excellent conductivity but extreme fragility, while a low content can produce soft and tough materials that fail to form a continuous conductive network, thereby limiting its conductivity. To address this challenge, Chong et al. employed a template-directed assembly strategy using poly(acrylic acid) (PAA) to organize PEDOT:PSS into a continuous nanofibrous conductive network through dimethyl sulfoxide (DMSO) treatment. The resulting PAA-templated hydrogel (T-ECH) combined tissue-like mechanical properties with a reported electrical conductivity of up to 247 S/cm (2.47×10^4 S/m). In contrast, the PAAm-templated control exhibited a conductivity of only 0.01 S/cm, highlighting the importance of template–PSS interactions in conductive network formation [84]. In another approach, He et al. polymerized pyrrole monomers *in situ* on the surface of nanofibers to form a conductive PPy layer. The material's conductivity and mechanical strength were significantly enhanced [177]. These studies demonstrate that conductivity is not solely proportional to the quantity of conductive additives but is critically influenced by the formation of internal conductive pathways, underscoring the need for sophisticated synthesis strategies.

5.2. Injectability and Self-Healing

Mechanical durability is essential for biomaterials intended for long-term applications such as tissue regeneration and drug delivery. If the conductive network is damaged or cracks appear in the implanted scaffold, the material's

conductivity, mechanical properties, and antibacterial performance may be compromised [178]. Consequently, researchers have designed hydrogels with self-healing properties to ensure mechanical durability *in vivo*.

The self-healing behavior of hydrogels is primarily achieved through reversible chemical covalent bonds and physical non-covalent interactions. Typical reversible chemical covalent bonds include imine bonds, hydrazone bonds, disulfide bonds, Diels-Alder reactions, and boronate-catechol complexes. In addition, physical non-covalent interactions can also provide self-healing properties to hydrogels, such as hydrophobic interactions, hydrogen bonds, electrostatic interactions, metal-ligand coordination, and π-π stacking [179]. Injectable hydrogels refer to hydrogels with shear-thinning properties, and generally, hydrogels with shear-thinning properties also possess self-healing capabilities. Injectable conductive hydrogels combine injectability with *in situ* gelation, enabling localized and minimally invasive delivery through narrow syringes, thereby avoiding invasive surgery. This approach significantly reduces patient discomfort, infection risks, recovery time, and treatment costs [180], making them highly promising for clinical applications.

Self-healing injectable electroactive hydrogels hold particular promise for hard tissue repair. For example, Wang et al. integrated a hybrid piezoelectric/triboelectric nanogenerator (HTP-NG) with a conductive hydrogel to construct an injectable symbiotic electrical stimulation system (BD-ES). The excellent injectability and adhesiveness of the hydrogel enable it to conform to bone defects of various shapes. The nanogenerator near the joint can harvest energy generated during patient-initiated or passive functional exercises, converting it into biphasic electrical pulses to induce osteogenic differentiation of stem cells, demonstrating promising potential for bone regeneration [136]. Due to the limited space around implants, self-healing injectable electroactive hydrogels can deliver sustained-release drugs to the gap between the implant and tissue under minimally invasive conditions. When designing these systems, a balance must be maintained between injectability/self-healing capabilities and physical stability/structural integrity. The incorporation of electroactive biomaterials (e.g., GO, CNTs, MXene, or piezoelectric ceramics) often significantly enhances mechanical properties [111]. Future research directions include precise control over piezoelectric characteristics, mechanical strength, and degradation kinetics, as well as the development of feedback-regulated systems that provide appropriate stimulation and support throughout the bone regeneration process.

6. Clinical Progress and Translational Challenges of Electroactive Biomaterials for Bone Repair

Although electroactive strategies have attracted substantial attention in preclinical bone regeneration research, their clinical translation remains uneven. Based on a targeted search of ClinicalTrials.gov and regulatory databases conducted on 26 March 2026, we did not identify registered phase I/II trials specifically evaluating implantable conductive or piezoelectric scaffolds for bone defect repair in humans. Instead, the clinically translated arm of "electroactive bone repair" is currently dominated by bone growth stimulation devices, including capacitive coupling (CC), pulsed electromagnetic fields (PEMF), combined magnetic fields (CMF), and low intensity pulsed ultrasound (LIPUS). FDA materials explicitly group these technologies as the main approved noninvasive bone growth stimulators, underscoring that clinical electroactivity has so far been realized primarily through devices rather than electroactive scaffolds [181].

Representative marketed products include Physio-Stim for established fracture nonunion, AccelStim as an FDA-approved LIPUS device for fracture healing, Xstim as an adjunct electrical treatment after primary lumbar spinal fusion, and the implantable direct-current SpF stimulator for spinal fusion. These examples demonstrate that electrical or electromechanical stimulation has already entered orthopedic practice, but mainly as external or implantable stimulators rather than biomaterial scaffolds.

Importantly, the clinical efficacy of electroactive stimulation is still indication-dependent and not uniformly convincing. A 2024 systematic review of randomized trials found that PEMF did not significantly improve acute fracture healing, highlighting the heterogeneity of treatment protocols and endpoints in current clinical evidence [182]. Thus, while electroactive concepts are clinically relevant, robust evidence remains stronger for selected indications such as nonunion management and spinal fusion adjunct therapy than for routine repair of critical-sized defects.

The major barriers to translation include the need for rigorous safety and efficacy evaluation, lengthy regulatory pathways, and the challenge of matching scaffold degradation with new bone formation while maintaining mechanical support and biocompatibility. Recent translational reviews of bone scaffolds also stress that clinical approval requires lifecycle evidence spanning feasibility testing, regulatory testing, manufacturing quality control, and prolonged follow-up. Therefore, future progress in electroactive bone biomaterials will likely depend on moving from proof-of-concept osteogenesis toward standardized electromechanical dosing, reproducible manufacturing, and well-designed first-in-human studies [183,184].

7. Summary and Outlook

The repair of bone defects has long posed a major clinical challenge. Electroactive biomaterials and the electrical cues they generate have demonstrated remarkable potential across multiple stages of bone healing, from promoting the migration, proliferation, and osteogenic differentiation of bone marrow mesenchymal stem cells to exerting antibacterial and immunomodulatory effects, and further regulating angiogenesis, neurogenesis, and bone tissue regeneration. From the perspective of the ERM, electroactive biomaterials function not merely as osteogenic scaffolds but as platforms for regulating the regenerative microenvironment through bioelectrical cues, thereby coordinating multiple biological processes involved in bone healing. Despite these advances, significant challenges remain in optimizing the interplay between biomaterials, donor cells, and the host microenvironment, as well as in translating experimental findings into clinically effective therapies.

Biocompatibility is a critical metric for the clinical transition of implantable biomaterials. For electroactive biomaterials, additional considerations including cellular tolerance to electrical stimulation, cell type–specific responses, systemic stress responses, and the propagation range of electrical stimulation need to be assessed. Although electroactive biomaterials can promote osteogenic differentiation of stem cells, further investigation is required to determine whether they inhibit the growth and proliferation of other cell types or trigger apoptosis, thereby ensuring their overall biosafety. These issues are closely related to the stability, safety, and controllability of the ERM engineered by electroactive biomaterials.

The electrophysiological environment of cells and tissues is highly intricate, and even minor changes in electrical stimulation can lead to different biological responses. It is crucial to clarify the interaction between electron-based electrical stimulation from electroactive biomaterials and ion-based electrical activity in organisms. It must be stressed that the effective voltage reaching the cell membrane is not only related to the electric field strength and electrode size but also depends on the conductivity of the biomaterial, the medium, and the electrical properties of the cell membrane [92]. Furthermore, the understanding of immune responses mediated by electroactive biomaterials [185], the feedback mechanisms of cells/tissues to electrical stimulation, and the involved intracellular signaling pathways remains incomplete. Continued investigation into these mechanisms is essential for establishing universal design principles for electroactive biomaterials and for defining safe, effective electrical stimulation parameters at the tissue, cellular, molecular, and genetic levels. Future research should focus on the precise engineering of electro-regenerative microenvironments, including spatial and temporal control of bioelectrical cues, multi-functional integration, and personalized regulation of the regenerative microenvironment. In summary, the development of electroactive biomaterials is evolving toward greater functionalization, precision, and diversification, urgently requiring researchers to innovate grounded in mechanistic insight and guided by real clinical needs.

Author Contributions

H.Y. and R.L.: Conceptualization, investigation, visualization, writing—original draft preparation; J.Z., Y.L. and K.C.: Investigation, writing—reviewing and editing; Y.Z., A.L. and C.H.: Conceptualization, supervision, writing—reviewing and editing. All authors have read and agreed to the published version of the manuscript.

Funding

This review was supported by the National Natural Science Foundation of China (82671293), the Fundamental Research Funds for the Central Universities (2042026kf0052), and open research fund of State Key Laboratory of Oral & Maxillofacial Reconstruction and Regeneration (2025KA09).

Institutional Review Board Statement

Not applicable.

Informed Consent Statement

Not applicable.

Data Availability Statement

No new datasets were generated or analyzed in this review. The literature discussed is cited in the reference list.

Conflicts of Interest

The authors declare no conflict of interests.

Use of AI and AI-Assisted Technologies

No AI tools were utilized for this paper.

References

1. Han, Y.; You, X.; Xing, W.; et al. Paracrine and endocrine actions of bone—The functions of secretory proteins from osteoblasts, osteocytes, and osteoclasts. *Bone Res.* **2018**, *6*, 16. https://doi.org/10.1038/s41413-018-0019-6.
2. Nan, S.; Yang, J.; Xie, Y.; et al. Bone function, dysfunction and its role in diseases including critical illness. *Int. J. Biol. Sci.* **2019**, *15*, 776–787. https://doi.org/10.7150/ijbs.27063.
3. Azi, M.L.; Aprato, A.; Santi, I.; et al. Autologous bone graft in the treatment of post-traumatic bone defects: A systematic review and meta-analysis. *BMC Musculoskelet. Disord.* **2016**, *17*, 465. https://doi.org/10.1186/s12891-016-1312-4.
4. Crane, G.M.; Ishaug, S.L.; Mikos, A.G. Bone tissue engineering. *Nat. Med.* **1995**, *1*, 1322–1324. https://doi.org/10.1038/nm1295-1322.
5. Rho, J.Y.; Kuhn-Spearing, L.; Zioupos, P. Mechanical properties and the hierarchical structure of bone. *Med. Eng. Phys.* **1998**, *20*, 92–102. https://doi.org/10.1016/s1350-4533(98)00007-1.
6. Chen, Y.; Wang, J.; Sun, J.; et al. Hierarchical structure and mechanical properties of remineralized dentin. *J. Mech. Behav. Biomed. Mater.* **2014**, *40*, 297–306. https://doi.org/10.1016/j.jmbbm.2014.08.024.
7. Khare, D.; Basu, B.; Dubey, A.K. Electrical stimulation and piezoelectric biomaterials for bone tissue engineering applications. *Biomaterials* **2020**, *258*, 120280. https://doi.org/10.1016/j.biomaterials.2020.120280.
8. Fu, F.; Wang, J.; Zeng, H.; et al. Functional Conductive Hydrogels for Bioelectronics. *ACS Mater. Lett.* **2020**, *2*, 1287–1301. https://doi.org/10.1021/acsmaterialslett.0c00309.
9. Jacob, J.; More, N.; Kalia, K.; et al. Piezoelectric smart biomaterials for bone and cartilage tissue engineering. *Inflamm. Regen.* **2018**, *38*, 2. https://doi.org/10.1186/s41232-018-0059-8.
10. Surmenev, R.A.; Orlova, T.; Chernozem, R.V.; et al. Hybrid lead-free polymer-based nanocomposites with improved piezoelectric response for biomedical energy-harvesting applications: A review. *Nano Energy* **2019**, *62*, 475–506. https://doi.org/10.1016/j.nanoen.2019.04.090.
11. Zhang, W.; Li, G.; Wang, B.; et al. Triboelectric Nanogenerators for Cellular Bioelectrical Stimulation. *Adv. Funct. Mater.* **2022**, *32*, 2203029. https://doi.org/10.1002/adfm.202203029.
12. Elsanadidy, E.; Mosa, I.M.; Luo, D.; et al. Advances in Triboelectric Nanogenerators for Self-powered Neuromodulation. *Adv. Funct. Mater.* **2023**, *33*, 2211177. https://doi.org/10.1002/adfm.202211177.
13. Parandeh, S.; Etemadi, N.; Kharaziha, M.; et al. Advances in Triboelectric Nanogenerators for Self-Powered Regenerative Medicine. *Adv. Funct. Mater.* **2021**, *31*, 2105169. https://doi.org/10.1002/adfm.202105169.
14. Lang, S.B. Pyroelectric Effect in Bone and Tendon. *Nature* **1966**, *212*, 704–705. https://doi.org/10.1038/212704a0.
15. Niu, Y.; Li, L.; Qi, Z.; et al. 0D van der Waals interfacial ferroelectricity. *Nat. Commun.* **2023**, *14*, 5578. https://doi.org/10.1038/s41467-023-41045-8.
16. Liu, Y.; McGuire, A.F.; Lou, H.Y.; et al. Soft conductive micropillar electrode arrays for biologically relevant electrophysiological recording. *Proc. Natl. Acad. Sci. USA* **2018**, *115*, 11718–11723. https://doi.org/10.1073/pnas.1810827115.
17. Gao, K.; Wu, N.; Ji, B.; et al. A Film Electrode upon Nanoarchitectonics of Bacterial Cellulose and Conductive Fabric for Forehead Electroencephalogram Measurement. *Sensors* **2023**, *23*, 7887. https://doi.org/10.3390/s23187887.
18. Liang, Y.; He, J.; Guo, B. Functional Hydrogels as Wound Dressing to Enhance Wound Healing. *ACS Nano* **2021**, *15*, 12687–12722. https://doi.org/10.1021/acsnano.1c04206.
19. Qiao, L.; Liang, Y.; Chen, J.; et al. Antibacterial conductive self-healing hydrogel wound dressing with dual dynamic bonds promotes infected wound healing. *Bioact. Mater.* **2023**, *30*, 129–141. https://doi.org/10.1016/j.bioactmat.2023.07.015.
20. Sinha, A.; Dhanjai; Stavrakis, A.K.; et al. Textile-based electrochemical sensors and their applications. *Talanta* **2022**, *244*, 123425. https://doi.org/10.1016/j.talanta.2022.123425.
21. Duan, Z.; Cai, F.; Chen, Y.; et al. Advanced Applications of Porous Materials in Triboelectric Nanogenerator Self-Powered Sensors. *Sensors* **2024**, *24*, 3812. https://doi.org/10.3390/s24123812.
22. Kim, D.; Han, S.A.; Kim, J.H.; et al. Biomolecular Piezoelectric Materials: From Amino Acids to Living Tissues. *Adv. Mater.* **2020**, *32*, 1906989. https://doi.org/10.1002/adma.201906989.
23. Luo, B.; Zhou, Q.; Chen, W.; et al. Nonadjacent Wireless Electrotherapy for Tissue Repair by a 3D-Printed Bioresorbable Fully Soft Triboelectric Nanogenerator. *Nano Lett.* **2023**, *23*, 2927–2937. https://doi.org/10.1021/acs.nanolett.3c00300.
24. Li, A.; Yang, J.; He, Y.; et al. Advancing piezoelectric 2D nanomaterials for applications in drug delivery systems and therapeutic approaches. *Nanoscale Horiz.* **2024**, *9*, 365–383. https://doi.org/10.1039/d3nh00578j.
25. Ikram, M.; Mahmud, M.A.P. Advanced triboelectric nanogenerator-driven drug delivery systems for targeted therapies. *Drug Deliv. Transl. Res.* **2023**, *13*, 54–78. https://doi.org/10.1007/s13346-022-01184-9.

26. Yuan, X.; Shi, J.; Kang, Y.; et al. Piezoelectricity, Pyroelectricity, and Ferroelectricity in Biomaterials and Biomedical Applications. *Adv. Mater.* **2024**, *36*, 2308726. https://doi.org/10.1002/adma.202308726.
27. Luo, S.; Zhang, C.; Xiong, W.; et al. Advances in electroactive biomaterials: Through the lens of electrical stimulation promoting bone regeneration strategy. *J. Orthop. Transl.* **2024**, *47*, 191–206. https://doi.org/10.1016/j.jot.2024.06.009.
28. Grosso, A.; Burger, M.G.; Lunger, A.; et al. It Takes Two to Tango: Coupling of Angiogenesis and Osteogenesis for Bone Regeneration. *Front. Bioeng. Biotechnol.* **2017**, *5*, 68. https://doi.org/10.3389/fbioe.2017.00068.
29. Su, N.; Villicana, C.; Yang, F. Immunomodulatory strategies for bone regeneration: A review from the perspective of disease types. *Biomaterials* **2022**, *286*, 121604. https://doi.org/10.1016/j.biomaterials.2022.121604.
30. Zhang, X.; Li, L.; Ouyang, J.; et al. Electroactive electrospun nanofibers for tissue engineering. *Nano Today* **2021**, *39*, 101196. https://doi.org/10.1016/j.nantod.2021.101196.
31. Wang, X.; Dai, X.; Chen, Y. Sonopiezoelectric Nanomedicine and Materdicine. *Small* **2023**, *19*, 2301693. https://doi.org/10.1002/smll.202301693.
32. Wang, J.; Lin, J.; Chen, L.; et al. Endogenous Electric-Field-Coupled Electrospun Short Fiber via Collecting Wound Exudation. *Adv. Mater.* **2022**, *34*, 2108325. https://doi.org/10.1002/adma.202108325.
33. Duolikun, D.; Zhang, L.; Wang, T.; et al. Bioelectric signals promote diabetic bone regeneration through Piezo1-mediated activation of the efferocytic immune microenvironment. *Bioact. Mater.* **2026**, *64*, 716–730. https://doi.org/10.1016/j.bioactmat.2026.05.037.
34. Reid, B.; Song, B.; Zhao, M. Electric currents in Xenopus tadpole tail regeneration. *Dev. Biol.* **2009**, *335*, 198–207. https://doi.org/10.1016/j.ydbio.2009.08.028.
35. Smith, R.S.; Walsh, C.A. Ion Channel Functions in Early Brain Development. *Trends Neurosci.* **2020**, *43*, 103–114. https://doi.org/10.1016/j.tins.2019.12.004.
36. Fukada, E.; Yasuda, I. On the Piezoelectric Effect of Bone. *J. Phys. Soc. Jpn.* **1957**, *12*, 1158–1162. https://doi.org/10.1143/jpsj.12.1158.
37. Ravi, H.K.; Simona, F.; Hulliger, J.; et al. Molecular Origin of Piezo- and Pyroelectric Properties in Collagen Investigated by Molecular Dynamics Simulations. *J. Phys. Chem. B* **2012**, *116*, 1901–1907. https://doi.org/10.1021/jp208436j.
38. Ramachandran, G.N.; Kartha, G. Structure of Collagen. *Nature* **1954**, *174*, 269–270. https://doi.org/10.1038/174269c0.
39. El Messiery, M.A.; Hastings, G.W.; Rakowski, S. Ferro-electricity of dry cortical bone. *J. Biomed. Eng.* **1979**, *1*, 63–65. https://doi.org/10.1016/0141-5425(79)90013-x.
40. Ravikumar, K.; Kumaran, V.; Basu, B. Biophysical implications of Maxwell stress in electric field stimulated cellular microenvironment on biomaterial substrates. *Biomaterials* **2019**, *209*, 54–66. https://doi.org/10.1016/j.biomaterials.2019.04.010.
41. Gommes, C.; Blacher, S.; Masenelli-Varlot, K.; et al. Image analysis characterization of multi-walled carbon nanotubes. *Carbon* **2003**, *41*, 2561–2572. https://doi.org/10.1016/s0008-6223(03)00375-0.
42. Moor, K.J.; Snow, S.D.; Kim, J.H. Differential Photoactivity of Aqueous [C_{60}] and [C_{70}] Fullerene Aggregates. *Environ. Sci. Technol.* **2015**, *49*, 5990–5998. https://doi.org/10.1021/acs.est.5b00100.
43. Wang, A.; Zhou, Y.; Wang, Z.; et al. Titanium incorporated with UiO-66(Zr)-type Metal–Organic Framework (MOF) for photocatalytic application. *RSC Adv.* **2016**, *6*, 3671–3679. https://doi.org/10.1039/c5ra24135a.
44. Wan, S.; Chen, Y.; Huang, C.; et al. Scalable ultrastrong MXene films with superior osteogenesis. *Nature* **2024**, *634*, 1103–1110. https://doi.org/10.1038/s41586-024-08067-8.
45. Adler, C.; Monavari, M.; Abraham, G.A.; et al. Mussel-inspired polydopamine decorated silane modified-electroconductive gelatin-PEDOT:PSS scaffolds for bone regeneration. *RSC Adv.* **2023**, *13*, 15960–15974. https://doi.org/10.1039/d3ra01311a.
46. Jin, L.; Tai, Y.; Nam, J. Piezoelectric silk fibroin nanofibers: Structural optimization to enhance piezoelectricity and biostability for neural tissue engineering. *Nano Energy* **2024**, *132*, 110367. https://doi.org/10.1016/j.nanoen.2024.110367.
47. Abdolmaleki, H.; Agarwala, S. PVDF-$BaTiO_3$ Nanocomposite Inkjet Inks with Enhanced β-Phase Crystallinity for Printed Electronics. *Polymers* **2020**, *12*, 2430. https://doi.org/10.3390/polym12102430.
48. Farooq, M.U.; Villaurrutia, R.; Maclaren, I.; et al. Using EBSD and TEM-Kikuchi patterns to study local crystallography at the domain boundaries of lead zirconate titanate. *J. Microsc.* **2008**, *230*, 445–454. https://doi.org/10.1111/j.1365-2818.2008.02004.x.
49. Shin, S.R.; Li, Y.C.; Jang, H.L.; et al. Graphene-based materials for tissue engineering. *Adv. Drug Deliv. Rev.* **2016**, *105*, 255–274. https://doi.org/10.1016/j.addr.2016.03.007.
50. Zhou, J.; Zhou, H.; Tang, J.; et al. Carbon dots doped with heteroatoms for fluorescent bioimaging: A review. *Microchim. Acta* **2017**, *184*, 343–368. https://doi.org/10.1007/s00604-016-2043-9.
51. Johnson, A.P.; Gangadharappa, H.V.; Pramod, K. Graphene nanoribbons: A promising nanomaterial for biomedical applications. *J. Control. Release* **2020**, *325*, 141–162. https://doi.org/10.1016/j.jconrel.2020.06.034.
52. Peng, Z.; Zhao, T.; Zhou, Y.; et al. Bone Tissue Engineering via Carbon-Based Nanomaterials. *Adv. Healthc. Mater.* **2020**, *9*, 1901495. https://doi.org/10.1002/adhm.201901495.

53. Kinloch, I.A.; Suhr, J.; Lou, J.; et al. Composites with carbon nanotubes and graphene: An outlook. *Science* **2018**, *362*, 547–553. https://doi.org/10.1126/science.aat7439.
54. Nascimento, L.; Fernandes, C.; Silva, R.M.; et al. Customizing 3D Structures of Vertically Aligned Carbon Nanotubes to Direct Neural Stem Cell Differentiation. *Adv. Healthc. Mater.* **2023**, *12*, 2300828. https://doi.org/10.1002/adhm.202300828.
55. Novoselov, K.S.; Geim, A.K.; Morozov, S.V.; et al. Electric Field Effect in Atomically Thin Carbon Films. *Science* **2004**, *306*, 666–669. https://doi.org/10.1126/science.1102896.
56. Ou, L.; Song, B.; Liang, H.; et al. Toxicity of graphene-family nanoparticles: A general review of the origins and mechanisms. *Part. Fibre Toxicol.* **2016**, *13*, 57. https://doi.org/10.1186/s12989-016-0168-y.
57. Cabral, C.S.D.; de Melo-Diogo, D.; Ferreira, P.; et al. Reduced graphene oxide–reinforced tricalcium phosphate/gelatin/chitosan light-responsive scaffolds for application in bone regeneration. *Int. J. Biol. Macromol.* **2024**, *259*, 129210. https://doi.org/10.1016/j.ijbiomac.2024.129210.
58. Feng, W.; Wang, Z. Biomedical applications of chitosan-graphene oxide nanocomposites. *iScience* **2022**, *25*, 103629. https://doi.org/10.1016/j.isci.2021.103629.
59. Fu, M.; Li, J.; Liu, M.; et al. Sericin/Nano-Hydroxyapatite Hydrogels Based on Graphene Oxide for Effective Bone Regeneration via Immunomodulation and Osteoinduction. *Int. J. Nanomed.* **2023**, *18*, 1875–1895. https://doi.org/10.2147/ijn.s399487.
60. Li, Y.; Yang, L.; Hou, Y.; et al. Polydopamine-mediated graphene oxide and nanohydroxyapatite-incorporated conductive scaffold with an immunomodulatory ability accelerates periodontal bone regeneration in diabetes. *Bioact. Mater.* **2022**, *18*, 213–227. https://doi.org/10.1016/j.bioactmat.2022.03.021.
61. Eivazzadeh-Keihan, R.; Maleki, A.; de la Guardia, M.; et al. Carbon based nanomaterials for tissue engineering of bone: Building new bone on small black scaffolds: A review. *J. Adv. Res.* **2019**, *18*, 185–201. https://doi.org/10.1016/j.jare.2019.03.011.
62. Sahithi, K.; Swetha, M.; Ramasamy, K.; et al. Polymeric composites containing carbon nanotubes for bone tissue engineering. *Int. J. Biol. Macromol.* **2010**, *46*, 281–283. https://doi.org/10.1016/j.ijbiomac.2010.01.006.
63. Hansen, S.F.; Lennquist, A. Carbon nanotubes added to the SIN List as a nanomaterial of Very High Concern. *Nat. Nanotechnol.* **2020**, *15*, 3–4. https://doi.org/10.1038/s41565-019-0613-9.
64. Gholizadeh, S.; Moztarzadeh, F.; Haghighipour, N.; et al. Preparation and characterization of novel functionalized multiwalled carbon nanotubes/chitosan/β-Glycerophosphate scaffolds for bone tissue engineering. *Int. J. Biol. Macromol.* **2017**, *97*, 365–372. https://doi.org/10.1016/j.ijbiomac.2016.12.086.
65. Lv, Y.; Wang, B.; Liu, G.; et al. Metal Material, Properties and Design Methods of Porous Biomedical Scaffolds for Additive Manufacturing: A Review. *Front. Bioeng. Biotechnol.* **2021**, *9*, 641130. https://doi.org/10.3389/fbioe.2021.641130.
66. Ma, S.; Song, K.; Lan, J.; et al. Biological and mechanical property analysis for designed heterogeneous porous scaffolds based on the refined TPMS. *J. Mech. Behav. Biomed. Mater.* **2020**, *107*, 103727. https://doi.org/10.1016/j.jmbbm.2020.103727.
67. Lin, H.; Shi, S.; Lan, X.; et al. Scaffold 3D-Printed from Metallic Nanoparticles-Containing Ink Simultaneously Eradicates Tumor and Repairs Tumor-Associated Bone Defects. *Small Methods* **2021**, *5*, 2100536. https://doi.org/10.1002/smtd.202100536.
68. Moon, K.S.; Park, Y.B.; Bae, J.M.; et al. Visible Light-Mediated Sustainable Antibacterial Activity and Osteogenic Functionality of Au and Pt Multi-Coated TiO_2 Nanotubes. *Materials* **2021**, *14*, 5976. https://doi.org/10.3390/ma14205976.
69. Eivazzadeh-Keihan, R.; Bahojb Noruzi, E.; Khanmohammadi Chenab, K.; et al. Metal-based nanoparticles for bone tissue engineering. *J. Tissue Eng. Regen. Med.* **2020**, *14*, 1687–1714. https://doi.org/10.1002/term.3131.
70. Mostafa, A.A.; El-Sayed, M.M.H.; Emam, A.N.; et al. Bioactive glass doped with noble metal nanoparticles for bone regeneration: *In Vitro* kinetics and proliferative impact on human bone cell line. *RSC Adv.* **2021**, *11*, 25628–25638. https://doi.org/10.1039/d1ra03876a.
71. Bim-Junior, O.; Alania, Y.; Tabatabaei, F.S.; et al. Biomimetic Growth of Metal–Organic Frameworks for the Stabilization of the Dentin Matrix and Control of Collagenolysis. *Langmuir* **2022**, *38*, 1600–1610. https://doi.org/10.1021/acs.langmuir.1c03073.
72. Naguib, M.; Kurtoglu, M.; Presser, V.; et al. Two-Dimensional Nanocrystals Produced by Exfoliation of Ti_3AlC_2. *Adv. Mater.* **2011**, *23*, 4248–4253. https://doi.org/10.1002/adma.201102306.
73. Ma, J.; Zhang, L.; Lei, B. Multifunctional MXene-Based Bioactive Materials for Integrated Regeneration Therapy. *ACS Nano* **2023**, *17*, 19526–19549. https://doi.org/10.1021/acsnano.3c01913.
74. Li, Z.; He, D.; Guo, B.; et al. Self-promoted electroactive biomimetic mineralized scaffolds for bacteria-infected bone regeneration. *Nat. Commun.* **2023**, *14*, 6963. https://doi.org/10.1038/s41467-023-42598-4.
75. Zhang, Y.; Li, Z.; Guo, B.; et al. A Zinc Oxide Nanowire-Modified Mineralized Collagen Scaffold Promotes Infectious Bone Regeneration. *Small* **2024**, *20*, 2309230. https://doi.org/10.1002/smll.202309230.

76. Lee, S.J.; Lee, H.J.; Kim, S.Y.; et al. *In Situ* gold nanoparticle growth on polydopamine-coated 3D-printed scaffolds improves osteogenic differentiation for bone tissue engineering applications: *In Vitro* and *in vivo* studies. *Nanoscale* **2018**, *10*, 15447–15453. https://doi.org/10.1039/c8nr04037k.
77. Ko, S.W.; Lee, J.Y.; Rezk, A.I.; et al. *In-Situ* cellulose-framework templates mediated monodispersed silver nanoparticles via facile UV-light photocatalytic activity for anti-microbial functionalization. *Carbohydr. Polym.* **2021**, *269*, 118255. https://doi.org/10.1016/j.carbpol.2021.118255.
78. Zhou, J.; Georgas, E.; Su, Y.; et al. Evolution from Bioinert to Bioresorbable: *In Vivo* Comparative Study of Additively Manufactured Metal Bone Scaffolds. *Adv. Sci.* **2023**, *10*, 2302702. https://doi.org/10.1002/advs.202302702.
79. Ghassemi, T.; Shahroodi, A.; Ebrahimzadeh, M.A.; et al. Current Concepts in Scaffolding for Bone Tissue Engineering. *Arch. Bone Jt. Surg.* **2018**, *6*, 90–99. https://doi.org/10.22038/abjs.2018.26340.1713.
80. Burnstine-Townley, A.; Eshel, Y.; Amdursky, N. Conductive Scaffolds for Cardiac and Neuronal Tissue Engineering: Governing Factors and Mechanisms. *Adv. Funct. Mater.* **2020**, *30*, 1901369. https://doi.org/10.1002/adfm.201901369.
81. Liu, D.; Wang, X.; Gao, C.; et al. Biodegradable Piezoelectric-Conductive Integrated Hydrogel Scaffold for Repair of Osteochondral Defects. *Adv. Mater.* **2024**, *36*, 2409400. https://doi.org/10.1002/adma.202409400.
82. Ravichandran, R.; Sundarrajan, S.; Venugopal, J.R.; et al. Applications of conducting polymers and their issues in biomedical engineering. *J. R. Soc. Interface* **2010**, *7*(Suppl. 5), S559–S579. https://doi.org/10.1098/rsif.2010.0120.focus.
83. Asri, N.A.N.; Mahat, M.M.; Zakaria, A.; et al. Fabrication Methods of Electroactive Scaffold-Based Conducting Polymers for Tissue Engineering Application: A Review. *Front. Bioeng. Biotechnol.* **2022**, *10*, 876696. https://doi.org/10.3389/fbioe.2022.876696.
84. Chong, J.; Sung, C.; Nam, K.S.; et al. Highly conductive tissue-like hydrogel interface through template-directed assembly. *Nat. Commun.* **2023**, *14*, 2206. https://doi.org/10.1038/s41467-023-37948-1.
85. Cheng, Y.C.; Chen, C.H.; Kuo, H.W.; et al. Electrical Stimulation through Conductive Substrate to Enhance Osteo-Differentiation of Human Dental Pulp-Derived Stem Cells. *Appl. Sci.* **2019**, *9*, 3938. https://doi.org/10.3390/app9183938.
86. Li, L.; Yu, D.; Li, J.; et al. Biodegradable Self-Enhancing Piezoelectric Scaffold for Synchronized Tendon-to-Bone Regeneration. *Adv. Mater.* **2026**, e74137. https://doi.org/10.1002/adma.74137.
87. Fan, B.; Guo, Z.; Li, X.; et al. Electroactive barium titanate coated titanium scaffold improves osteogenesis and osseointegration with low-intensity pulsed ultrasound for large segmental bone defects. *Bioact. Mater.* **2020**, *5*, 1087–1101. https://doi.org/10.1016/j.bioactmat.2020.07.001. Erratum in *Bioact. Mater.* **2024**, *40*, 275–279. https://doi.org/10.1016/j.bioactmat.2024.06.006.
88. Bai, Y.; Dai, X.; Yin, Y.; et al. Biomimetic piezoelectric nanocomposite membranes synergistically enhance osteogenesis of deproteinized bovine bone grafts. *Int. J. Nanomed.* **2019**, *14*, 3015–3026. https://doi.org/10.2147/ijn.s197824.
89. Lai, C.; Cheng, M.; Ning, C.; et al. Janus electro-microenvironment membrane with surface-selective osteogenesis/gingival healing ability for guided bone regeneration. *Mater. Today Bio* **2022**, *17*, 100491. https://doi.org/10.1016/j.mtbio.2022.100491.
90. Zhang, X.; Zhang, C.; Lin, Y.; et al. Nanocomposite Membranes Enhance Bone Regeneration through Restoring Physiological Electric Microenvironment. *ACS Nano* **2016**, *10*, 7279–7286. https://doi.org/10.1021/acsnano.6b02247.
91. Wang, Z.L.; Song, J. Piezoelectric Nanogenerators Based on Zinc Oxide Nanowire Arrays. *Science* **2006**, *312*, 242–246. https://doi.org/10.1126/science.1124005.
92. Murillo, G.; Blanquer, A.; Vargas-Estevez, C.; et al. Electromechanical Nanogenerator–Cell Interaction Modulates Cell Activity. *Adv. Mater.* **2017**, *29*, 1605048. https://doi.org/10.1002/adma.201605048.
93. Laurenti, M.; Cauda, V. ZnO Nanostructures for Tissue Engineering Applications. *Nanomaterials* **2017**, *7*, 374. https://doi.org/10.3390/nano7110374.
94. Vannozzi, L.; Gouveia, P.; Pingue, P.; et al. Novel Ultrathin Films Based on a Blend of PEG-*b*-PCL and PLLA and Doped with ZnO Nanoparticles. *ACS Appl. Mater. Interfaces* **2020**, *12*, 21398–21410. https://doi.org/10.1021/acsami.0c00154.
95. Lang, S.B.; Tofail, S.A.M.; Kholkin, A.L.; et al. Ferroelectric Polarization in Nanocrystalline Hydroxyapatite Thin Films on Silicon. *Sci. Rep.* **2013**, *3*, 2215. https://doi.org/10.1038/srep02215.
96. Góes, J.C.; Figueiró, S.D.; de Paiva, J.A.C.; et al. Piezoelectric and dielectric properties of collagen films. *Phys. Status Solidi A* **1999**, *176*, 1077–1083. https://doi.org/10.1002/(sici)1521-396x(199912)176:2<1077::aid-pssa1077>3.0.co;2-f.
97. Zhou, Z.; Qian, D.; Minary-Jolandan, M. Molecular Mechanism of Polarization and Piezoelectric Effect in Super-Twisted Collagen. *ACS Biomater. Sci. Eng.* **2016**, *2*, 929–936. https://doi.org/10.1021/acsbiomaterials.6b00021.
98. Silva, C.C.; Pinheiro, A.G.; Thomazini, D.; et al. Effect of the pH on the piezoelectric properties of collagen films. *Mater. Sci. Eng. B* **2001**, *83*, 165–172. https://doi.org/10.1016/s0921-5107(01)00520-7.
99. Silva, C.C.; Pinheiro, A.G.; Figueiró, S.D.; et al. Piezoelectric properties of collagen-nanocrystalline hydroxyapatite composites. *J. Mater. Sci.* **2002**, *37*, 2061–2070. https://doi.org/10.1023/a:1015219800490.
100. Ma, B.; Liu, F.; Li, Z.; et al. Piezoelectric nylon-11 nanoparticles with ultrasound assistance for high-efficiency promotion of stem cell osteogenic differentiation. *J. Mater. Chem. B* **2019**, *7*, 1847–1854. https://doi.org/10.1039/c8tb03321h.

101. Donate, R.; Paz, R.; Moriche, R.; et al. An overview of polymeric composite scaffolds with piezoelectric properties for improved bone regeneration. *Mater. Des.* **2023**, *231*, 112085. https://doi.org/10.1016/j.matdes.2023.112085.
102. Mirzaei, A.; Saburi, E.; Enderami, S.E.; et al. Synergistic effects of polyaniline and pulsed electromagnetic field to stem cells osteogenic differentiation on polyvinylidene fluoride scaffold. *Artif. Cells Nanomed. Biotechnol.* **2019**, *47*, 3058–3066. https://doi.org/10.1080/21691401.2019.1645154.
103. Zheng, T.; Yu, Y.; Pang, Y.; et al. Improving bone regeneration with composites consisting of piezoelectric poly(l-lactide) and piezoelectric calcium/manganese co-doped barium titanate nanofibers. *Compos. Part B Eng.* **2022**, *234*, 109734. https://doi.org/10.1016/j.compositesb.2022.109734.
104. Joo, S.; Gwon, Y.; Kim, S.; et al. Piezoelectrically and Topographically Engineered Scaffolds for Accelerating Bone Regeneration. *ACS Appl. Mater. Interfaces* **2024**, *16*, 1999–2011. https://doi.org/10.1021/acsami.3c12575.
105. Huang, Z.X.; Li, L.W.; Huang, Y.Z.; et al. Self-poled piezoelectric polymer composites via melt-state energy implantation. *Nat. Commun.* **2024**, *15*, 819. https://doi.org/10.1038/s41467-024-45184-4.
106. Dai, X.; Yao, X.; Zhang, W.; et al. The Osteogenic Role of Barium Titanate/Polylactic Acid Piezoelectric Composite Membranes as Guiding Membranes for Bone Tissue Regeneration. *Int. J. Nanomed.* **2022**, *17*, 4339–4353. https://doi.org/10.2147/ijn.s378422.
107. Balikov, D.A.; Fang, B.; Chun, Y.W.; et al. Directing lineage specification of human mesenchymal stem cells by decoupling electrical stimulation and physical patterning on unmodified graphene. *Nanoscale* **2016**, *8*, 13730–13739. https://doi.org/10.1039/c6nr04400j.
108. Hou, Y.; Wang, W.; Bartolo, P. The effect of graphene and graphene oxide induced reactive oxygen species on polycaprolactone scaffolds for bone cancer applications. *Mater. Today Bio* **2024**, *24*, 100886. https://doi.org/10.1016/j.mtbio.2023.100886.
109. Li, P.; Xu, T.; Dang, X.; et al. Improving astaxanthin-loaded chitosan/polyvinyl alcohol/graphene oxide nanofiber membranes and their application in periodontitis. *Int. J. Biol. Macromol.* **2024**, *258*, 128980. https://doi.org/10.1016/j.ijbiomac.2023.128980.
110. Xue, H.; Zhang, Z.; Lin, Z.; et al. Enhanced tissue regeneration through immunomodulation of angiogenesis and osteogenesis with a multifaceted nanohybrid modified bioactive scaffold. *Bioact. Mater.* **2022**, *18*, 552–568. https://doi.org/10.1016/j.bioactmat.2022.05.023.
111. Chopra, V.; Thomas, J.; Kaushik, S.; et al. Injectable Bone Cement Reinforced with Gold Nanodots Decorated rGO-Hydroxyapatite Nanocomposites, Augment Bone Regeneration. *Small* **2023**, *19*, 2204637. https://doi.org/10.1002/smll.202204637.
112. An, N.; Yan, X.; Qiu, Q.; et al. Human periodontal ligament stem cell sheets activated by graphene oxide quantum dots repair periodontal bone defects by promoting mitochondrial dynamics dependent osteogenic differentiation. *J. Nanobiotechnol.* **2024**, *22*, 133. https://doi.org/10.1186/s12951-024-02422-7.
113. Liu, X.; George, M.N.; Park, S.; et al. 3D-printed scaffolds with carbon nanotubes for bone tissue engineering: Fast and homogeneous one-step functionalization. *Acta Biomater.* **2020**, *111*, 129–140. https://doi.org/10.1016/j.actbio.2020.04.047.
114. Zhu, S.; Jing, W.; Hu, X.; et al. Time-dependent effect of electrical stimulation on osteogenic differentiation of bone mesenchymal stromal cells cultured on conductive nanofibers. *J. Biomed. Mater. Res. Part A* **2017**, *105*, 3369–3383. https://doi.org/10.1002/jbm.a.36181.
115. Ghimire, U.; Jang, S.R.; Adhikari, J.R.; et al. Conducting biointerface of spider-net-like chitosan-adorned polyurethane/SPIONs@SrO_2–fMWCNTs for bone tissue engineering and antibacterial efficacy. *Int. J. Biol. Macromol.* **2024**, *264*, 130602. https://doi.org/10.1016/j.ijbiomac.2024.130602.
116. Huang, Y.; Zhang, L.; Ji, Y.; et al. A non-invasive smart scaffold for bone repair and monitoring. *Bioact. Mater.* **2023**, *19*, 499–510. https://doi.org/10.1016/j.bioactmat.2022.04.034.
117. Huang, Y.; Jing, W.; Li, Y.; et al. Composites made of polyorganophosphazene and carbon nanotube up-regulating osteogenic activity of BMSCs under electrical stimulation. *Colloids Surf. B Biointerfaces* **2021**, *204*, 111785. https://doi.org/10.1016/j.colsurfb.2021.111785.
118. Liu, X.; George, M.N.; Li, L.; et al. Injectable Electrical Conductive and Phosphate Releasing Gel with Two-Dimensional Black Phosphorus and Carbon Nanotubes for Bone Tissue Engineering. *ACS Biomater. Sci. Eng.* **2020**, *6*, 4653–4665. https://doi.org/10.1021/acsbiomaterials.0c00612.
119. Lee, H.; Cho, Y. An Innovative Strategy for the Fabrication of Functional Cell Sheets Using an Electroactive Conducting Polymer. *Theranostics* **2015**, *5*, 1021–1029. https://doi.org/10.7150/thno.12389.
120. Dutta, S.D.; Ganguly, K.; Randhawa, A.; et al. Electrically stimulated 3D bioprinting of gelatin-polypyrrole hydrogel with dynamic semi-IPN network induces osteogenesis via collective signaling and immunopolarization. *Biomaterials* **2023**, *294*, 121999. https://doi.org/10.1016/j.biomaterials.2023.121999.
121. Zhou, T.; Yan, L.; Xie, C.; et al. A Mussel-Inspired Persistent ROS-Scavenging, Electroactive, and Osteoinductive Scaffold Based on Electrochemical-Driven *In Situ* Nanoassembly. *Small* **2019**, *15*, 1805440. https://doi.org/10.1002/smll.201805440.
122. Wu, C.; He, X.; Zhu, Y.; et al. Electrochemical deposition of Ppy/Dex/ECM coatings and their regulation on cellular responses through electrical controlled drug release. *Colloids Surf. B Biointerfaces* **2023**, *222*, 113016. https://doi.org/10.1016/j.colsurfb.2022.113016.

123. Chen, J.; Yu, M.; Guo, B.; et al. Conductive nanofibrous composite scaffolds based on in-situ formed polyaniline nanoparticle and polylactide for bone regeneration. *J. Colloid Interface Sci.* **2018**, *514*, 517–527. https://doi.org/10.1016/j.jcis.2017.12.062.
124. Yu, C.; Ying, X.; Shahbazi, M.A.; et al. A nano-conductive osteogenic hydrogel to locally promote calcium influx for electro-inspired bone defect regeneration. *Biomaterials* **2023**, *301*, 122266. https://doi.org/10.1016/j.biomaterials.2023.122266.
125. Huang, Y.; Du, Z.; Zheng, T.; et al. Antibacterial, conductive, and osteocompatible polyorganophosphazene microscaffolds for the repair of infectious calvarial defect. *J. Biomed. Mater. Res. Part A* **2021**, *109*, 2580–2596. https://doi.org/10.1002/jbm.a.37252.
126. Hu, Z.C.; Lu, J.Q.; Zhang, T.W.; et al. Piezoresistive MXene/Silk fibroin nanocomposite hydrogel for accelerating bone regeneration by Re-establishing electrical microenvironment. *Bioact. Mater.* **2023**, *22*, 1–17. https://doi.org/10.1016/j.bioactmat.2022.08.025.
127. Wang, H.; Hsu, Y.C.; Wang, C.; et al. Conductive and Enhanced Mechanical Strength of $Mo_2Ti_2C_3$MXene-Based Hydrogel Promotes Neurogenesis and Bone Regeneration in Bone Defect Repair. *ACS Appl. Mater. Interfaces* **2024**, *16*, 17208–17218. https://doi.org/10.1021/acsami.3c19410.
128. Xi, Y.; Pan, W.; Xi, D.; et al. Optimization, characterization and evaluation of ZnO/polyvinylidene fluoride nanocomposites for orthopedic applications: Improved antibacterial ability and promoted osteoblast growth. *Drug Deliv.* **2020**, *27*, 1378–1385. https://doi.org/10.1080/10717544.2020.1827084.
129. Sikder, P.; Nagaraju, P.; Naganaboyina, H.P.S. 3D-Printed Piezoelectric Porous Bioactive Scaffolds and Clinical Ultrasonic Stimulation Can Help in Enhanced Bone Regeneration. *Bioengineering* **2022**, *9*, 679. https://doi.org/10.3390/bioengineering9110679.
130. Li, G.; Li, Z.; Min, Y.; et al. 3D-Printed Piezoelectric Scaffolds with Shape Memory Polymer for Bone Regeneration. *Small* **2023**, *19*, 2302927. https://doi.org/10.1002/smll.202302927.
131. Zheng, T.; Pang, Y.; Zhang, D.; et al. Integrated Piezoelectric/Conductive Composite Cryogel Creates Electroactive Microenvironment for Enhanced Bone Regeneration. *Adv. Healthc. Mater.* **2023**, *12*, 2300927. https://doi.org/10.1002/adhm.202300927.
132. Wu, H.; Dong, H.; Tang, Z.; et al. Electrical stimulation of piezoelectric $BaTiO_3$ coated Ti_6Al_4V scaffolds promotes anti-inflammatory polarization of macrophages and bone repair via MAPK/JNK inhibition and OXPHOS activation. *Biomaterials* **2023**, *293*, 121990. https://doi.org/10.1016/j.biomaterials.2022.121990.
133. Zhao, Y.; Cai, Y.; Wang, W.; et al. Periosteum-bone inspired hierarchical scaffold with endogenous piezoelectricity for neuro-vascularized bone regeneration. *Bioact. Mater.* **2025**, *44*, 339–353. https://doi.org/10.1016/j.bioactmat.2024.10.020.
134. Mao, L.; Zhang, D.; Shen, Z.; et al. Recombinant human bone morphogenetic protein-2-engineered piezoplatform synergistically promotes bone regeneration through bone morphogenetic protein receptor activation. *Biomater. Transl.* **2025**, *6*, 450–464. https://doi.org/10.12336/bmt.25.00019.
135. Wang, K.; Jiang, K. A Periosteum-Inspired Janus Piezoelectric Scaffold Using Bioenergetic-Driven H-Type Vascularization for Diabetic Bone Regeneration. *Adv. Sci.* **2026**, *13*, e75948. https://doi.org/10.1002/advs.75948.
136. Wang, T.; Ouyang, H.; Luo, Y.; et al. Rehabilitation exercise–driven symbiotic electrical stimulation system accelerating bone regeneration. *Sci. Adv.* **2024**, *10*, eadi6799. https://doi.org/10.1126/sciadv.adi6799.
137. Xu, C.; Long, Y.; Feng, L.; et al. Bionic Triboelectric Nanogenerator Activates the "mechano-electro-biochemical" Cascade Effect *In Situ* to Accelerate Critical-Sized Bone Defect Repair. *Adv. Mater.* **2025**, *37*, 2504128. https://doi.org/10.1002/adma.202504128.
138. Wang, B.; Li, G.; Zhu, Q.; et al. Bone Repairment via Mechanosensation of Piezo1 Using Wearable Pulsed Triboelectric Nanogenerator. *Small* **2022**, *18*, 2201056. https://doi.org/10.1002/smll.202201056.
139. Kao, F.C.; Chiu, P.Y.; Tsai, T.T.; et al. The application of nanogenerators and piezoelectricity in osteogenesis. *Sci. Technol. Adv. Mater.* **2019**, *20*, 1103–1117. https://doi.org/10.1080/14686996.2019.1693880.
140. Swain, S.; Padhy, R.N.; Rautray, T.R. Polarized piezoelectric bioceramic composites exhibit antibacterial activity. *Mater. Chem. Phys.* **2020**, *239*, 122002. https://doi.org/10.1016/j.matchemphys.2019.122002.
141. Xu, W.; Yu, Y.; Li, K.; et al. Surface-Confined Piezocatalysis Inspired by ROS Generation of Mitochondria Respiratory Chain for Ultrasound-Driven Noninvasive Elimination of Implant Infection. *ACS Nano* **2023**, *17*, 9415–9428. https://doi.org/10.1021/acsnano.3c01480.
142. Li, K.; Xu, W.; Chen, Y.; et al. Piezoelectric Nanostructured Surface for Ultrasound-Driven Immunoregulation to Rescue Titanium Implant Infection. *Adv. Funct. Mater.* **2023**, *33*, 2214522. https://doi.org/10.1002/adfm.202214522.
143. Li, M.; Li, H.; Pan, Q.; et al. Graphene Oxide and Lysozyme Ultrathin Films with Strong Antibacterial and Enhanced Osteogenesis. *Langmuir* **2019**, *35*, 6752–6761. https://doi.org/10.1021/acs.langmuir.9b00035.
144. Sun, J.; Xu, C.; Wo, K.; et al. Wireless Electric Cues Mediate Autologous DPSC-Loaded Conductive Hydrogel Microspheres to Engineer the Immuno-Angiogenic Niche for Homologous Maxillofacial Bone Regeneration. *Adv. Healthc. Mater.* **2024**, *13*, 2303405. https://doi.org/10.1002/adhm.202303405.

145. Adamopoulos, I.E. Inflammation in bone physiology and pathology. *Curr. Opin. Rheumatol.* **2018**, *30*, 59–64. https://doi.org/10.1097/bor.0000000000000449.
146. Halaney, D.L.; Zahedivash, A.; Phipps, J.E.; et al. Differences in forward angular light scattering distributions between M1 and M2 macrophages. *J. Biomed. Opt.* **2015**, *20*, 115002. https://doi.org/10.1117/1.jbo.20.11.115002.
147. Roy Barman, S.; Jhunjhunwala, S. Electrical Stimulation for Immunomodulation. *ACS Omega* **2024**, *9*, 52–66. https://doi.org/10.1021/acsomega.3c06696.
148. Jiang, Y.; Zhao, W.; Xu, S.; et al. Bioinspired design of mannose-decorated globular lysine dendrimers promotes diabetic wound healing by orchestrating appropriate macrophage polarization. *Biomaterials* **2022**, *280*, 121323. https://doi.org/10.1016/j.biomaterials.2021.121323.
149. Kong, Y.; Liu, F.; Ma, B.; et al. Wireless Localized Electrical Stimulation Generated by an Ultrasound-Driven Piezoelectric Discharge Regulates Proinflammatory Macrophage Polarization. *Adv. Sci.* **2021**, *8*, 2100962. https://doi.org/10.1002/advs.202100962.
150. Li, C.; Zhang, S.; Yao, Y.; et al. Piezoelectric Bioactive Glasses Composite Promotes Angiogenesis by the Synergistic Effect of Wireless Electrical Stimulation and Active Ions. *Adv. Healthc. Mater.* **2023**, *12*, 2300064. https://doi.org/10.1002/adhm.202300064.
151. Wang, Y.; Li, W.; Guo, Y.; et al. Mitochondria Transplantation to Bone Marrow Stromal Cells Promotes Angiogenesis During Bone Repair. *Adv. Sci.* **2024**, *11*, 2403201. https://doi.org/10.1002/advs.202403201.
152. Fan, Y.; Sun, J.; Fan, W.; et al. Three-Dimensional Semiconductor Network as Regulators of Energy Metabolism Drives Angiogenesis in Bone Regeneration. *ACS Nano* **2024**, *18*, 32602–32616. https://doi.org/10.1021/acsnano.4c09971. Correction in: *ACS Nano* **2025**, *19*, 17950–17951. https://doi.org/10.1021/acsnano.5c05619.
153. Wang, L.; Pang, Y.; Tang, Y.; et al. A biomimetic piezoelectric scaffold with sustained Mg^{2+} release promotes neurogenic and angiogenic differentiation for enhanced bone regeneration. *Bioact. Mater.* **2023**, *25*, 399–414. https://doi.org/10.1016/j.bioactmat.2022.11.004.
154. Koo, J.; MacEwan, M.R.; Kang, S.K.; et al. Wireless bioresorbable electronic system enables sustained nonpharmacological neuroregenerative therapy. *Nat. Med.* **2018**, *24*, 1830–1836. https://doi.org/10.1038/s41591-018-0196-2.
155. Lu, S.; Chen, W.; Wang, J.; et al. Polydopamine-Decorated PLCL Conduit to Induce Synergetic Effect of Electrical Stimulation and Topological Morphology for Peripheral Nerve Regeneration. *Small Methods* **2023**, *7*, 2200883. https://doi.org/10.1002/smtd.202200883.
156. Han, F.; Ma, X.; Zhai, Y.; et al. Strategy for Designing a Cell Scaffold to Enable Wireless Electrical Stimulation for Enhanced Neuronal Differentiation of Stem Cells. *Adv. Healthc. Mater.* **2021**, *10*, 2100027. https://doi.org/10.1002/adhm.202100027.
157. Sun, L.; Xiong, F.; Gong, B.; et al. Nanofiber-Based Electroactive Interfaces Enabling Coordinated Neuromodulation and Peripheral Nerve Regeneration. *Adv. Mater.* **2026**, *38*, e72880. https://doi.org/10.1002/adma.72880.
158. Su, Y.; Zeng, L.; Deng, R.; et al. Endogenous Electric Field-Coupled PD@BP Biomimetic Periosteum Promotes Bone Regeneration through Sensory Nerve via Fanconi Anemia Signaling Pathway. *Adv. Healthc. Mater.* **2023**, *12*, 2203027. https://doi.org/10.1002/adhm.202203027.
159. Qin, W.; Li, L.; Niu, W.; et al. Effects of Electric Field-Modulated Conductive Hydrogel on Osseoperception and Osseointegration of Dental Implants. *Adv. Funct. Mater.* **2024**, *34*, 2400256. https://doi.org/10.1002/adfm.202400256.
160. Mi, J.; Xu, J.K.; Yao, Z.; et al. Implantable Electrical Stimulation at Dorsal Root Ganglions Accelerates Osteoporotic Fracture Healing via Calcitonin Gene-Related Peptide. *Adv. Sci.* **2022**, *9*, 2103005. https://doi.org/10.1002/advs.202103005.
161. Jing, X.; Xu, C.; Su, W.; et al. Photosensitive and Conductive Hydrogel Induced Innerved Bone Regeneration for Infected Bone Defect Repair. *Adv. Healthc. Mater.* **2023**, *12*, 2201349. https://doi.org/10.1002/adhm.202201349.
162. Huang, K.; Li, Z.; Lin, J.; et al. Two-dimensional transition metal carbides and nitrides (MXenes) for biomedical applications. *Chem. Soc. Rev.* **2018**, *47*, 5109–5124. https://doi.org/10.1039/c7cs00838d. Correction in: *Chem. Soc. Rev.* **2018**, *47*, 6889. https://doi.org/10.1039/C8CS90090F.
163. Fu, Y.; Zhang, J.; Lin, H.; et al. 2D titanium carbide(MXene) nanosheets and 1D hydroxyapatite nanowires into free standing nanocomposite membrane: *In Vitro* and *in vivo* evaluations for bone regeneration. *Mater. Sci. Eng. C* **2021**, *118*, 111367. https://doi.org/10.1016/j.msec.2020.111367.
164. Zhang, X.; Wang, T.; Zhang, Z.; et al. Electrical stimulation system based on electroactive biomaterials for bone tissue engineering. *Mater. Today* **2023**, *68*, 177–203. https://doi.org/10.1016/j.mattod.2023.06.011.
165. Dubey, A.K.; Basu, B. Pulsed Electrical Stimulation and Surface Charge Induced Cell Growth on Multistage Spark Plasma Sintered Hydroxyapatite-Barium Titanate Piezobiocomposite. *J. Am. Ceram. Soc.* **2014**, *97*, 481–489. https://doi.org/10.1111/jace.12647.
166. Li, J.; Mou, X.; Qiu, J.; et al. Surface Charge Regulation of Osteogenic Differentiation of Mesenchymal Stem Cell on Polarized Ferroelectric Crystal Substrate. *Adv. Healthc. Mater.* **2015**, *4*, 998–1003. https://doi.org/10.1002/adhm.201500032.
167. Li, G.; Zhu, Q.; Wang, B.; et al. Rejuvenation of Senescent Bone Marrow Mesenchymal Stromal Cells by Pulsed Triboelectric Stimulation. *Adv. Sci.* **2021**, *8*, 2100964. https://doi.org/10.1002/advs.202100964.

168. Tian, J.; Shi, R.; Liu, Z.; et al. Self-powered implantable electrical stimulator for osteoblasts' proliferation and differentiation. *Nano Energy* **2019**, *59*, 705–714. https://doi.org/10.1016/j.nanoen.2019.02.073.
169. Yao, G.; Kang, L.; Li, C.; et al. A self-powered implantable and bioresorbable electrostimulation device for biofeedback bone fracture healing. *Proc. Natl. Acad. Sci. USA* **2021**, *118*, e2100772118. https://doi.org/10.1073/pnas.2100772118.
170. Xiao, X.; Meng, X.; Kim, D.; et al. Ultrasound-Driven Injectable and Fully Biodegradable Triboelectric Nanogenerators. *Small Methods* **2023**, *7*, 2201350. https://doi.org/10.1002/smtd.202201350.
171. Liu, T.; Liu, M.; Dou, S.; et al. Triboelectric-Nanogenerator-Based Soft Energy-Harvesting Skin Enabled by Toughly Bonded Elastomer/Hydrogel Hybrids. *ACS Nano* **2018**, *12*, 2818–2826. https://doi.org/10.1021/acsnano.8b00108.
172. Zhang, J.; Hu, Y.; Lin, X.; et al. High-performance triboelectric nanogenerator based on chitin for mechanical-energy harvesting and self-powered sensing. *Carbohydr. Polym.* **2022**, *291*, 119586. https://doi.org/10.1016/j.carbpol.2022.119586.
173. Qin, C.; Lu, A. Flexible, anti-freezing self-charging power system composed of cellulose based supercapacitor and triboelectric nanogenerator. *Carbohydr. Polym.* **2021**, *274*, 118667. https://doi.org/10.1016/j.carbpol.2021.118667.
174. Chen, K.; Chen, Y.; Deng, Q.; et al. Strong and biocompatible poly(lactic acid) membrane enhanced by Ti_3C_2Tz (MXene) nanosheets for Guided bone regeneration. *Mater. Lett.* **2018**, *229*, 114–117. https://doi.org/10.1016/j.matlet.2018.06.063.
175. Yu, X.; Wang, X.; Li, D.; et al. Mechanically reinforced injectable bioactive nanocomposite hydrogels for in-situ bone regeneration. *Chem. Eng. J.* **2022**, *433*, 132799. https://doi.org/10.1016/j.cej.2021.132799.
176. Yang, T.; Deng, W.; Tian, G.; et al. Modulating piezoelectricity and mechanical strength via three-dimensional gradient structure for piezoelectric composites. *Mater. Horiz.* **2023**, *10*, 5045–5052. https://doi.org/10.1039/d3mh00603d.
177. He, H.; Li, H.; Pu, A.; et al. Hybrid assembly of polymeric nanofiber network for robust and electronically conductive hydrogels. *Nat. Commun.* **2023**, *14*, 759. https://doi.org/10.1038/s41467-023-36438-8.
178. Tu, Y.; Chen, N.; Li, C.; et al. Advances in injectable self-healing biomedical hydrogels. *Acta Biomater.* **2019**, *90*, 1–20. https://doi.org/10.1016/j.actbio.2019.03.057.
179. Bertsch, P.; Diba, M.; Mooney, D.J.; et al. Self-Healing Injectable Hydrogels for Tissue Regeneration. *Chem. Rev.* **2023**, *123*, 834–873. https://doi.org/10.1021/acs.chemrev.2c00179.
180. Bakaic, E.; Smeets, N.M.B.; Hoare, T. Injectable hydrogels based on poly(ethylene glycol) and derivatives as functional biomaterials. *RSC Adv.* **2015**, *5*, 35469–35486. https://doi.org/10.1039/c4ra13581d.
181. U.S. Food and Drug Administration. *Physical Medicine Devices; Reclassification of Non-Invasive Bone Growth Stimulators*; U.S. Food and Drug Administration: Silver Spring, MD, USA, 2026; Vol. 91, pp. 20352–20362.
182. Picelli, A.; Di Censo, R.; Tomasello, S.; et al. Effects of pulsed electromagnetic fields on bone fractures: A systematic review update. *Eur. J. Phys. Rehabil. Med.* **2024**, *60*, 989–994. https://doi.org/10.23736/s1973-9087.24.08226-1.
183. Zhao, X.; Li, N.; Zhang, Z.; et al. Beyond hype: Unveiling the Real challenges in clinical translation of 3D printed bone scaffolds and the fresh prospects of bioprinted organoids. *J. Nanobiotechnol.* **2024**, *22*, 500. https://doi.org/10.1186/s12951-024-02759-z.
184. Shen, N.; Zhang, Z.; Wu, F.; et al. Advances in self-powered biomaterials for bone defect repair. *Adv. Compos. Hybrid Mater.* **2025**, *8*, 38. https://doi.org/10.1007/s42114-024-01115-x.
185. Lee, J.; Byun, H.; Madhurakkat Perikamana, S.K.; et al. Current Advances in Immunomodulatory Biomaterials for Bone Regeneration. *Adv. Healthc. Mater.* **2019**, *8*, 1801106. https://doi.org/10.1002/adhm.201801106.